AEDC-TR-69-199

INVESTIGATION OF LAMINAR BOUNDARY-LAYER SEPARATION ON A FLAT-PLATE-RAMP COMBINATION WITH AND WITHOUT MASS REMOVAL AT MACH NUMBERS 6, 8, AND 10

R. W. Rhudy

ARO, Inc.

March 1970

VON KÁRMÁN GAS DYNAMICS FACILITY
ARNOLD ENGINEERING DEVELOPMENT CENTER
AIR FORCE SYSTEMS COMMAND
ARNOLD AIR FORCE STATION, TENNESSEE

NOTICES

INVESTIGATION OF LAMINAR BOUNDARY-LAYER SEPARATION ON A FLAT-PLATE-RAMP COMBINATION WITH AND WITHOUT MASS REMOVAL AT MACH NUMBERS 6, 8, AND 10

R. W. Rhudy

ARO, Inc.

FOREWORD

The work reported was done at the request of the Air Force Flight Dynamics Laboratory (AFFDL), Flight Mechanics Division, Air Force Systems Command (AFSC), under Program Element 62201F, Project 1366.

The results of the tests presented were obtained by ARO, Inc. (a subsidiary of Sverdrup & Parcel and Associates, Inc.), contract operator of the Arnold Engineering Development Center (AEDC), AFSC, Arnold Air Force Station, Tennessee, under Contract F40600-69-C-0001. The tests were conducted from July 11, 1965, to April 18, 1969, under ARO Project No. VT0611, and the manuscript was submitted for publication on August 8, 1969.

The author wishes to acknowledge the contributions of Mr. J. D. Gray, who supplied the theoretical calculations presented herein.

This technical report has been reviewed and is approved.

Eugene C. Fletcher
Lt Colonel, USAF
AF Representative, VKF
Directorate of Test

Roy R. Croy, Jr.
Colonel, USAF
Director of Test

ABSTRACT

An experimental investigation of laminar boundary-layer separation induced by a trailing edge ramp on a flat plate was conducted at Mach numbers of 6, 8, and 10. The tests were conducted over a range of Reynolds numbers. Longitudinal and spanwise surface pressure distributions, pitot pressure profiles, and shadowgraph pictures were used to investigate the two-dimensionality of the flow and the effects of model geometry, angle of attack, Reynolds number, ramp angle, and mass removal from the separation region. Data are presented to show that laminar, two-dimensional boundary-layer reattachment, not limited by model geometry, was obtained. These data are compared to the integral-moment theory of Lees and Reeves as modified by Klineberg. It is also shown that a separation region can be reduced or even eliminated by removing mass at the hinge line.

CONTENTS

ILLUSTRATIONS

TABLES

NOMENCLATURE

b	Flat-plate semi-span, in.
C	Chapman-Rubesin viscosity factor, $(T/T_w)(\mu_w/\mu)$
C_p	Pressure coefficient $(p - p_\infty)/q_\infty$
d	Bleed slot opening in streamwise direction, in. or ft
h	Total enthalpy, Btu-lb^{-1}-°R^{-1}
M	Mach number
p	Static pressure, psia or psfa
q	Dynamic pressure, psia
Re	Unit Reynolds number, in.$^{-1}$ or ft^{-1}
S_w	Total enthalpy function, $(h_w/h_L - 1)$
T	Temperature, °R
u	Velocity, ft-sec^{-1}
$\dot{W}_B$	Weight flow bleed per unit span, $0.532\ p_c d\ T_w^{-1/2}$, lb-ft^{-1}-sec^{-1}
$\dot{W}_T$	Theoretical weight flow per unit span in laminar boundary layer at x_c, $_0\int^\delta \rho_L u_L dy$, lb-ft^{-1}-sec^{-1}
x	Streamwise surface distance measured from leading edge, in.
y	Vertical height measured normal to surface, in.

z	Spanwise distance from model centerline, in.
α_M	Angle between flat plate and free stream, deg
δ	Boundary-layer thickness, in.
θ	Angle between ramp and flat plate, deg
θ_S	Angle between oblique shock wave and flat plate, deg
μ	Dynamic viscosity, lb-sec-ft^{-2}
ρ	Density, lb-ft^{-3}
$\overline{\chi}$	Hypersonic viscous interaction parameter, $M_{w_i}^3 \left[C_\infty / (Re_x)_{w_i} \right]^{1/2}$

SUBSCRIPTS

b	Model base value
c	Value at ramp leading edge
i	Local inviscid value
L	Local conditions within the boundary layer
NB	Value with no bleed
o	Value at start of interaction
t	Tunnel stilling chamber conditions
w	Model wall conditions
x	Value based on length x
∞	Free-stream conditions

SECTION I
INTRODUCTION

An experimental study was conducted to investigate the effects of mass removal (bleed) on two-dimensional, laminar boundary-layer separation. The test program, supported by the Air Force Flight Dynamics Laboratory, was undertaken to determine the feasibility of increasing hypersonic control surface effectiveness by reducing the extent of separation caused by a deflected control surface. The program was expected to verify and extend, over a wider range of Mach numbers and Reynolds numbers, the mass bleed studies of Ball (Ref. 1).

The primary criteria for these tests were that the flow be: (1) laminar through reattachment, (2) two-dimensional over a finite span each side of the model centerline, and (3) the reattachment location must not be limited by the ramp length. In order to provide information that the above criteria could be met, extensive "no bleed" tests were conducted at Mach numbers 6, 8, and 10 and several Reynolds numbers. Because the results in Ref. 2 showed that large ramp angles would probably trigger transition during flow reattachment, the tests were conducted using a nominal ramp angle of 10 deg. During these initial tests, data were obtained to check the feasibility of pitching the model to obtain a Mach number lower than free stream on the plate. Checks were also made early in the tests, with the model unpitched, to determine if the separation extent could be reduced by venting the separation region to the model base pressure.

A model support failure during model injection at M_∞ = 6 made further testing at this time impractical. Because of the failure, very little data were obtained with mass bleed; however, the groundwork has been done for future investigation of this concept.

The tests were run at free-stream Mach numbers of 6, 8, and 10 and Reynolds numbers, based on the length from the leading edge to hinge line, from 0.19×10^6 to 1.5×10^6. Data, some of which were with side plates installed on the model, were obtained for pitch angles from 0 to 18 deg and with ramp angles of zero and approximately 10 deg. Tests were made with slot openings of 0.062 and 0.125 in. at M_∞ = 8.

1

SECTION II
APPARATUS

2.1 WIND TUNNELS

The tunnels (Gas Dynamic Wind Tunnels, Hypersonic (B) and (C)) are continuous, closed-circuit, variable density wind tunnels with axisymmetric contoured nozzles and 50-in.-diam test sections. Tunnel B was operated at a nominal Mach number of 6 or 8 at stagnation pressures from 27 to 110 and from 90 to 420 psia, respectively, at stagnation temperatures up to 1280°R. Tunnel C was operated at a nominal Mach number of 10 at stagnation pressure from 210 to 840 psia at 1900°R stagnation temperature. The model may be injected into the tunnels for a test run and then retracted for model cooling or model changes without interrupting the tunnel flow.

2.2 MODEL

The model, furnished by AFFDL, (Fig. 1) was a sharp leading-edge flat plate with a hinged trailing-edge ramp. The hinge provided for ramp angles from 0 to 30 deg, although tests were conducted only at zero and approximately 10 deg. A full-span channel extending (internally) from just ahead of the hinge line (0.125 in.) to the base of the model provided for mass removal, i.e., "bleed." Sharp-lip inserts were used in the entrance of the channel to vary the full-span slot opening from 0 to 0.125 in., in the streamwise direction. Because early data indicated that the extent of boundary-layer separation was limited by ramp length, an extension was built by VKF to lengthen the ramp from 4.5 to 9.0 in. All subsequent tests were run with this extension in place. The base of the model was shielded from the support yoke by a fairing plate extending downstream from the model, Fig. 1. Lower surface side plates were an integral part of the model support. The built-in angle between the axis of the yoke and the upper surface (25 deg), along with the other mounting equipment, provided for upper surface pitch angles from 0 to 30 deg with respect to the free-stream flow. An additional fairing plate was added to the lower surface of the yoke during testing in an attempt to reduce tunnel choking presumed to be caused by the strong bow wave ahead of the yoke.
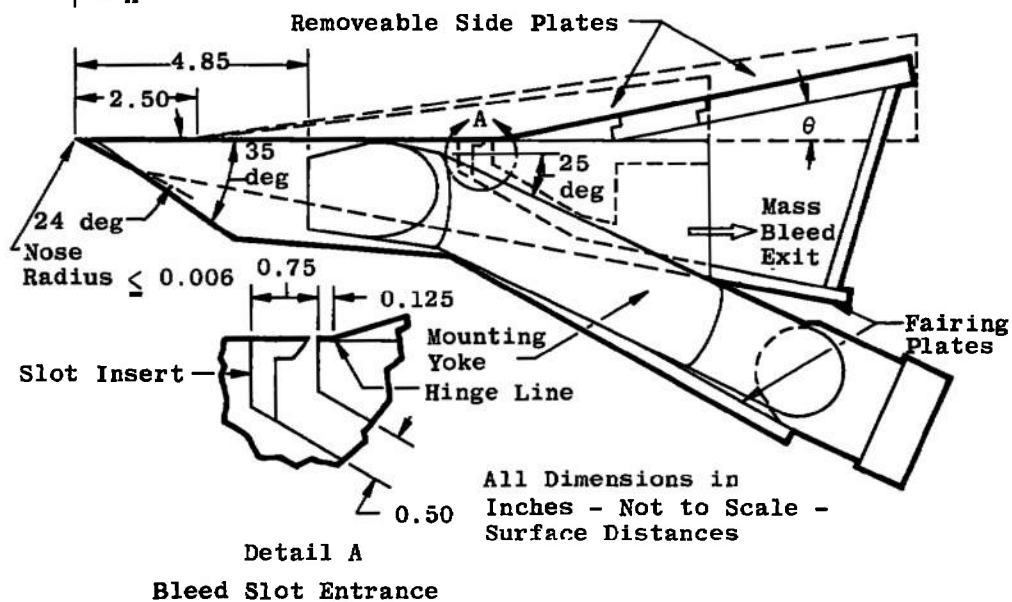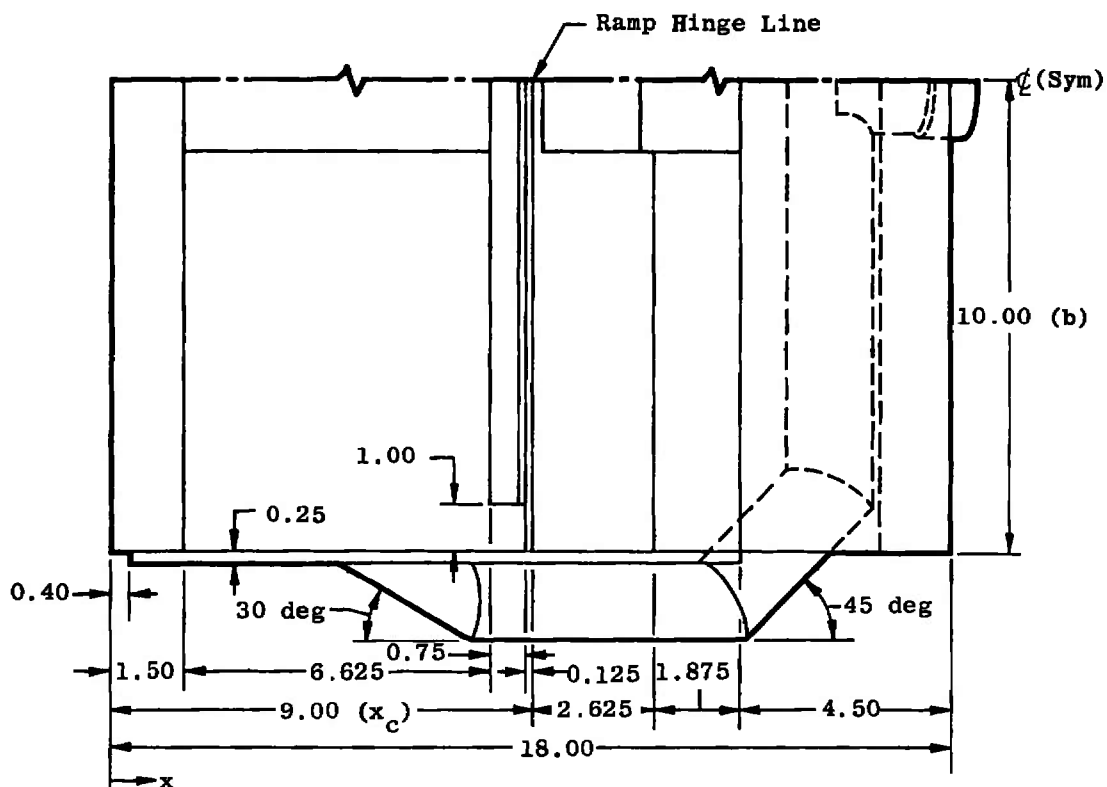
a. Dimensions

Fig. 1 Model Details

3

Alignment of the model in pitch was within ±0.1 deg; however, because of the clutch face on the yoke, the model was rolled 0.25 deg. This small roll angle, when combined with angle of attack, created a slight leading-edge yaw (less than 0.25 deg).

Removable side plates (Fig. 1), which extended from near the leading edge of the flat plate to the trailing edge of the ramp (a set for both ramp lengths), were mounted on the outboard edge of the plate during some of the tests.

The model was instrumented with surface pressure taps (0.062-in. ID) as shown in Fig. 2. In addition to the centerline row on the flat plate, two closely spaced orifice rows were located 4 in. toward on side and 7 in. toward the other side to provide a detailed check of the longitudinal pressure distribution off axis. Three spanwise rows, at $x/x_c = 0.5$, 0.72 and 0.89, were also provided for checking the pressure variation in a lateral direction. Three thermocouples, mounted in pressure orifices, were used to monitor the plate surface temperature.

AEDC
11885-68
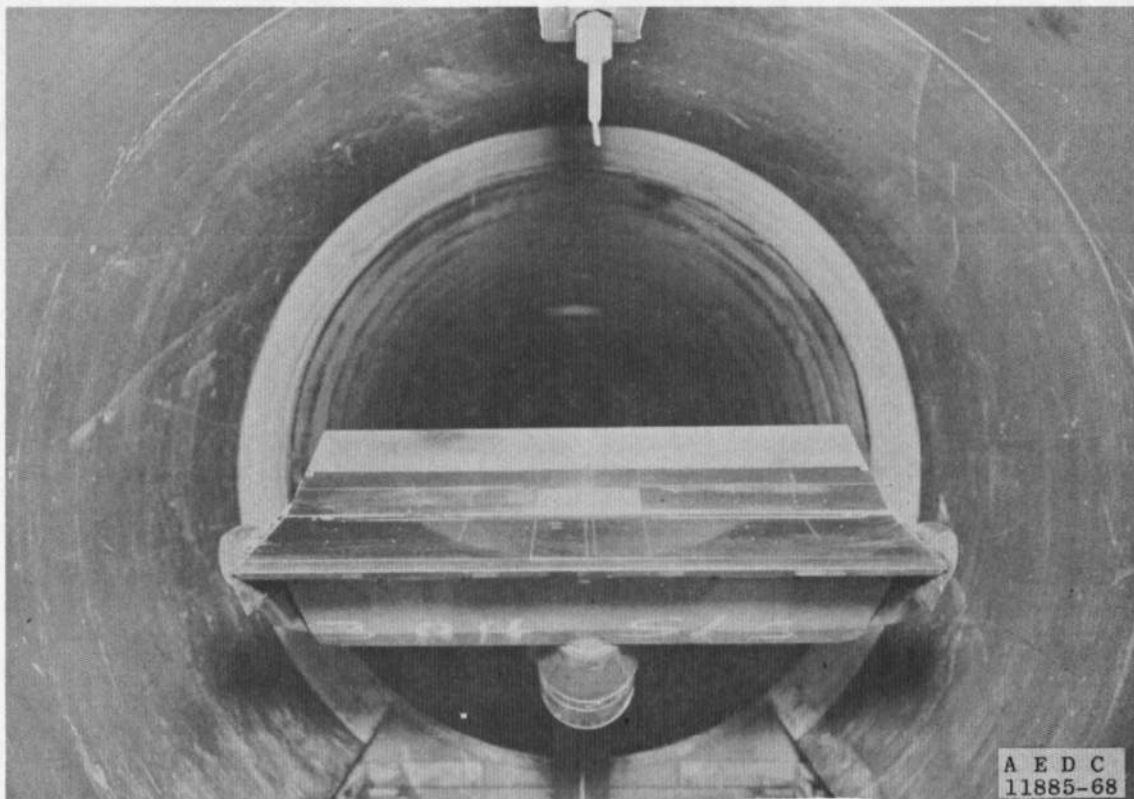
b. Model Installed in Hypersonic Tunnel

Fig. 1 Concluded
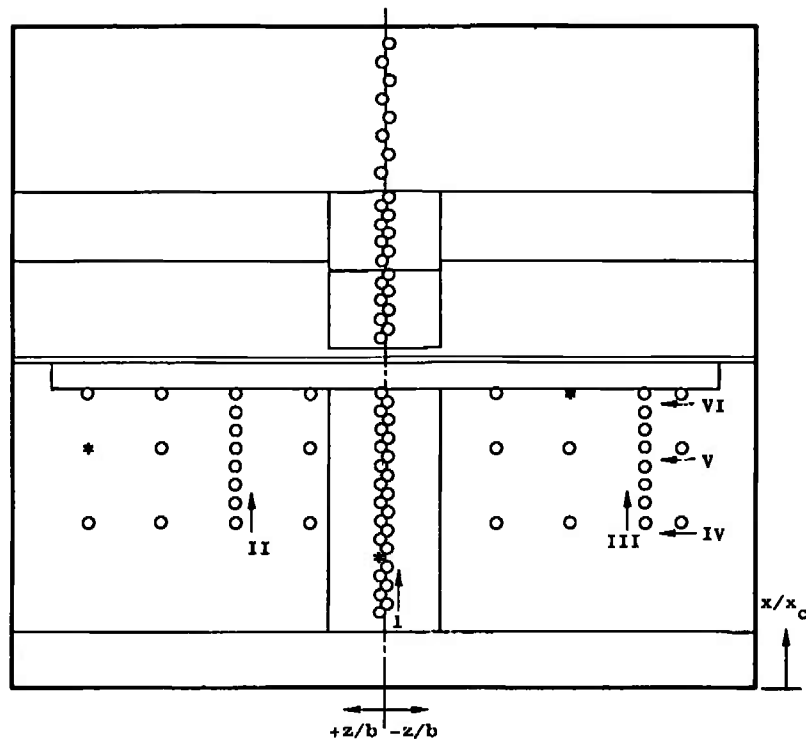
Row	Tap	x/x_c	z/b
I	1	0.222	±0.012
	2	0.250	
	3	0.278	
	4	0.306	
	5	0.333	
	6	0.362	
	7*	0.389	
	8	0.417	
	9	0.444	
	10	0.472	
	11	0.500	
	12	0.528	
	13	0.555	
	14	0.584	
	15	0.610	
	16	0.639	
	17	0.667	
	18	0.694	
	19	0.722	
	20	0.750	
	21	0.777	
	22	0.806	
	23	0.834	
	24	0.861	
	25	0.888	
	26	1.056	
	27	1.083	
	28	1.111	
	29	1.140	
	30	1.167	
	31	1.194	
	32	1.223	
	33	1.251	
	34	1.307	
	35	1.335	
	36	1.361	
	37	1.389	
	38	1.416	
	39	1.443	
	40	1.474	
	41	1.498	
	42	1.555	
	43	1.611	
	44	1.668	
	45	1.722	
	46	1.778	
	47	1.833	
	48	1.890	
	49	1.945	

Row	Tap	x/x_c	z/b
II	50	0.500	0.400
	51	0.555	
	52	0.610	
	53	0.667	
	54	0.722	
	55	0.777	
	56	0.834	
	57	0.888	
III	59	0.500	-0.700
	60	0.555	
	61	0.610	
	62	0.667	
	63	0.722	
	64	0.777	
	65	0.834	
	66	0.888	
IV	67	0.500	-0.800
	59		-0.700
	68		-0.500
	69		-0.300
	11		+0.012
	70		0.200
	50		0.400
	71		0.600
	72		0.800
V	73	0.722	-0.800
	63		-0.700
	74		-0.500
	75		-0 300
	19		+0.012
	76		0.200
	54		0.400
	77		0.600
	78*		0.800
VI	79	0.888	-0.800
	66		-0.700
	80*		-0.500
	81		-0.300
	25		+0.012
	82		0.200
	57		0.400
	83		0.600
	84		0.800

* Surface Thermocouple

b = Semi-span ~ 10 in.

x_c = Distance from L.E. to Hinge Line ~ 9.0 in.

Fig. 2 Instrumentation Locations

2.3 INSTRUMENTATION

Model pressures were measured in Tunnel B with 1-psid trans-
ducers on the forward plate and 15-psid transducers on the ramp. In
Tunnel C, 1- and 15-psid transducers were switched in and out of the
system automatically to allow measuring to the best precision. All
transducers were referenced to near vacuum. From repeat calibra-
tions, the estimated Tunnel B pressure measurement precision was
±0.001 psi or ±0.5 percent, whichever was greater, for the 1-psid
transducer and ±0.003 psi or ±0.5 percent, whichever was greater,
for the 15-psid transducers. The estimated Tunnel C precision was
±0.001 psi or ±0.5 percent, whichever was greater.

The precision of the temperature measurements, using
Chromel®-Alumel® thermocouples, was ±2°F or ±0.5 percent, which-
ever was greater.

The pitot pressure measurements were made with a 0.012-in.-
high oval probe connected to a 15-psid transducer. The probe drive
allowed the probe to travel normal to the surface of the ramp with an
estimated precision of ±0.001 in. in the y direction. The estimated
precision of the probe pressure was ±0.003 psi or ±0.5 percent, which-
ever was greater. Model flow field shadowgraphs were obtained during
all tests.

SECTION III
PROCEDURE

The tests were conducted at nominal free-stream Mach numbers
of 6, 8, and 10 with Reynolds numbers, based on the length to the hinge
line, from 0.19 x 10^6 to 1.5 x 10^6. The test conditions are shown in
Table I.

The local flow conditions when the model was pitched were obtained
from the curves in the Appendix. These curves were calculated from
the information contained in Ref. 3. A complete test summary is shown
in Table II.

TABLE I
TEST CONDITIONS

Nominal M_∞	P_t, psia	T_t, °R	M_∞	$Re_\infty \times 10^{-6}$, ft.$^{-1}$
6	27	850	5.96	0.50
	54		5.98	1.00
	72		6.00	1.33
	110		6.02	2.00
8	90	1140	7.87	0.50
	195	1210	7.92	1.00
	270	1240	7.94	1.33
	420	1280	7.97	2.00
10	210	1900	9.93	0.25
	420		10.01	0.50
	840		10.09	1.00

TABLE II
TEST SUMMARY

a. Surface Pressure Distributions

Nominal M_{W_1}	Nominal M_∞	$Re_{x_C} \times 10^{-6}$	θ, deg	α_M, deg	Ramp Length, x/x_C	d, in.	Side Plates
4.4	8	0.40	0	18.0	1.5	0	Off
4.5	6	1.5, 1.0, 0.75	10	6.4	1.5	0	Off
	8	1.0	10	16.4	1.5	0.062 and 0.125	Off
	6	1.5, 1.0, 0.75	10	11.0	1.5	0	On
	6	1.5	10	11.0	1.5	0	Off
	6	1.5, 0.75	11	11.0	2.0	0	Off
5.8	8	0.58	0	10.0	1.5	0	Off
5.0	8	1.5, 1.0, 0.75	10	8.8	1.5	0	Off
	6	1.5, 1.0	10	8.8	1.5	0.062	Off
	8	1.5	10	8.9	1.5	0.125	Off
	6	1.5, 1.0, 0.75	10	0	1.5	0	On and Off
	6	1.5, 0.75, 0.38	11	0	2.0	0	Off
	6	0.38	11	0	2.0	0	On
6.6	8	0.54	0	6.0	1.5	0	Off
8.0	8	0.38	0	0	1.5	0	Off
	8	1.5, 0.75, 0.38	10	0	1.5	0	Off
	8	0.75	10	0	1.5	0	On
	6	1.0, 0.75	10	0	1.5	0, 0.062, 0.125	Off
	6	0.38	10.5	0	2.0	0	Off
	8	0.38, 0.75	11	0	2.0	0	On and Off
10.0	10	0.38, 0.75, 1.5	9.5	0	2.0	0	On
	10	0.19, 0.38, 0.75	10.5	0	2.0	0	On
	10	0.19, 0.38, 0.75	11	0	2.0	0	On

b. Pitot Pressure Surveys

Ramp, x/x_C = 2.0			θ = 11.0 deg	d = 0	α_M = 0
M_{W_1}	M_∞	$Re_{x_C} \times 10^{-6}$	x/x_C	z/b	Side Plates
6.0	6	0.38	1.47	0, ±0.4	On and Off
	6	0.38	1.47	-0.7	Off
	6	0.75	1.47 and 1.84	0, ±0.4, -0.7	Off
	6	1.50	1.84	0, ±0.4, -0.7	Off
8.0	8	0.38	1.47 and 1.84	0, ±0.4, -0.7	On and Off
	8	0.75	1.47	0, ±0.4, -0.7	Off
	8	0.75	1.84	0, -0.4	Off

The boundary-layer pitot pressure data were taken at two stream-wise positions on the ramp (x/x_c = 1.47 and 1.84) and several (z/b = 0, ±0.4, and 0.7) spanwise locations by surveying normal to the surface of the ramp. The measurements were used along with a measured ramp surface static pressure, which was assumed constant through the boundary layer, to calculate the local Mach number. Selected data were repeated with the side plates installed.

The forward plate temperature, which was monitored during all tests, in general was near an equilibrium condition being 0.88 T_t at Mach number 6, 0.78 T_t at Mach number 8, and 0.72 T_t at Mach number 10.

<div align="center">

SECTION IV
RESULTS AND DISCUSSION

</div>

4.1 TWO-DIMENSIONALITY OF THE FLOW

In order to demonstrate that a laminar, two-dimensional separation that was not influenced by the model geometry limitations could be obtained, the initial investigations were conducted with mass bleed channel sealed. Data were also obtained with the ramp at zero deflection for reference purposes. The flat-plate pressure is shown in Fig. 3 in terms of the variation in the ratio of measured pressure to the inviscid wedge pressure (obtained from curves in the Appendix) as a function of the hypersonic viscous interaction parameter, $\bar{\chi}$. These data were obtained at several angles of attack at a fixed free-stream unit Reynolds number (Re_∞ = 0.5 x 10^6 ft^{-1}). The data agree reasonably well with the weak interaction formula of Ref. 4.

An indication of the two-dimensionality of the flow over the plate with a deflected ramp is shown in Figs. 4 through 6. The pressure distributions for M_{w_i} = 6 (Fig. 4a) show a pronounced discrepancy between the centerline data and that from the off-centerline rows, especially with the side plates removed. This discrepancy is most pronounced in the region of the maximum pressure gradient. The spanwise pressure distributions (Fig. 4b) also show this variation in pressure between centerline and the off centerline. From these figures, it appears that the upstream influence of the ramp, i.e., the start of the pressure rise, was less off centerline than on. The ramp boundary-layer profiles (Fig. 4c) indicate that reattachment occured earlier outboard of the centerline (z/b = 0) because higher Mach numbers were measured close to the ramp surface. This is consistent with a reduction in upstream influence.

There was little change in the profiles with the side plates removed. The choice of static pressure used for data reduction was the reason that some of the curves do not go to a Mach number ratio of zero in the recirculation region. The proper static pressure would only shift the curves to the left or right and would not change the overall trend.
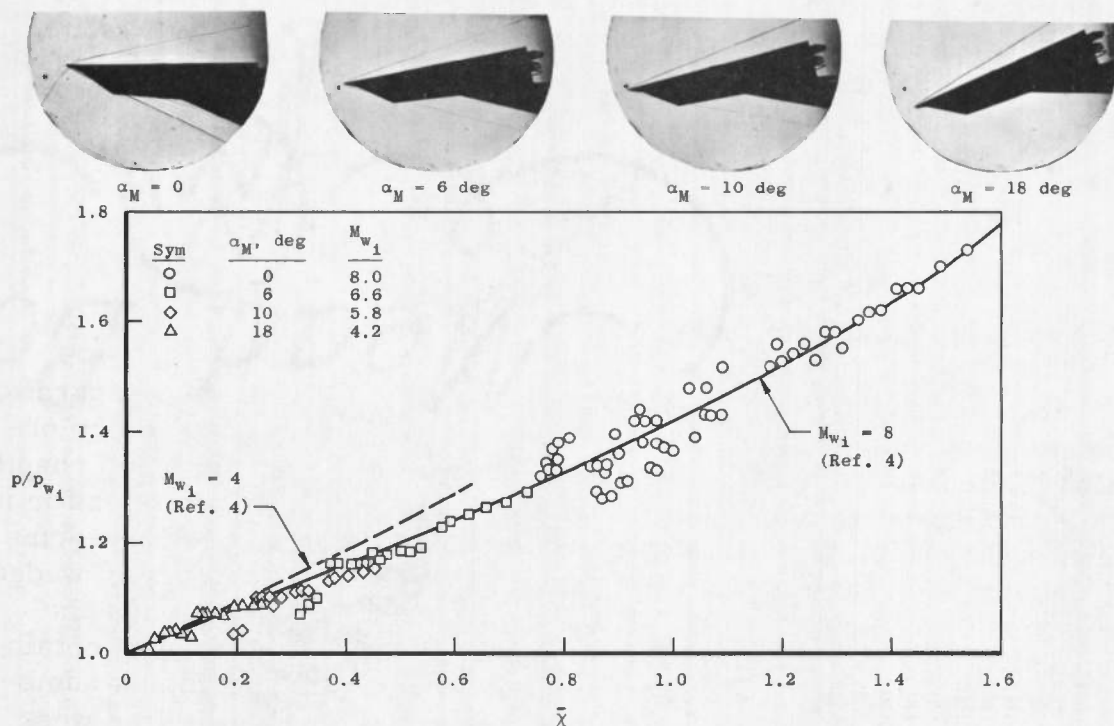

Fig. 3 Flat-Plate Correlation at $M_\infty = 8$, $Re_\infty = 0.5 \times 10^{-6}$, ft^{-1}

When all of the data are considered, the flow appears to be two-dimensional on the centerline, but only for a small span on each side, e.g., $z/b \approx \pm 0.1$. This is based on the fact that (1) the centerline data were unaffected by the removal of the side plates, and (2) they agree well with the VKF calculations based on the integral-moment theory of Ref. 5 as modified in Ref. 4 ($S_w = 0$). The discrepancy between theory and experiment on the downstream part of the ramp is discussed in detail in Section 4.4.
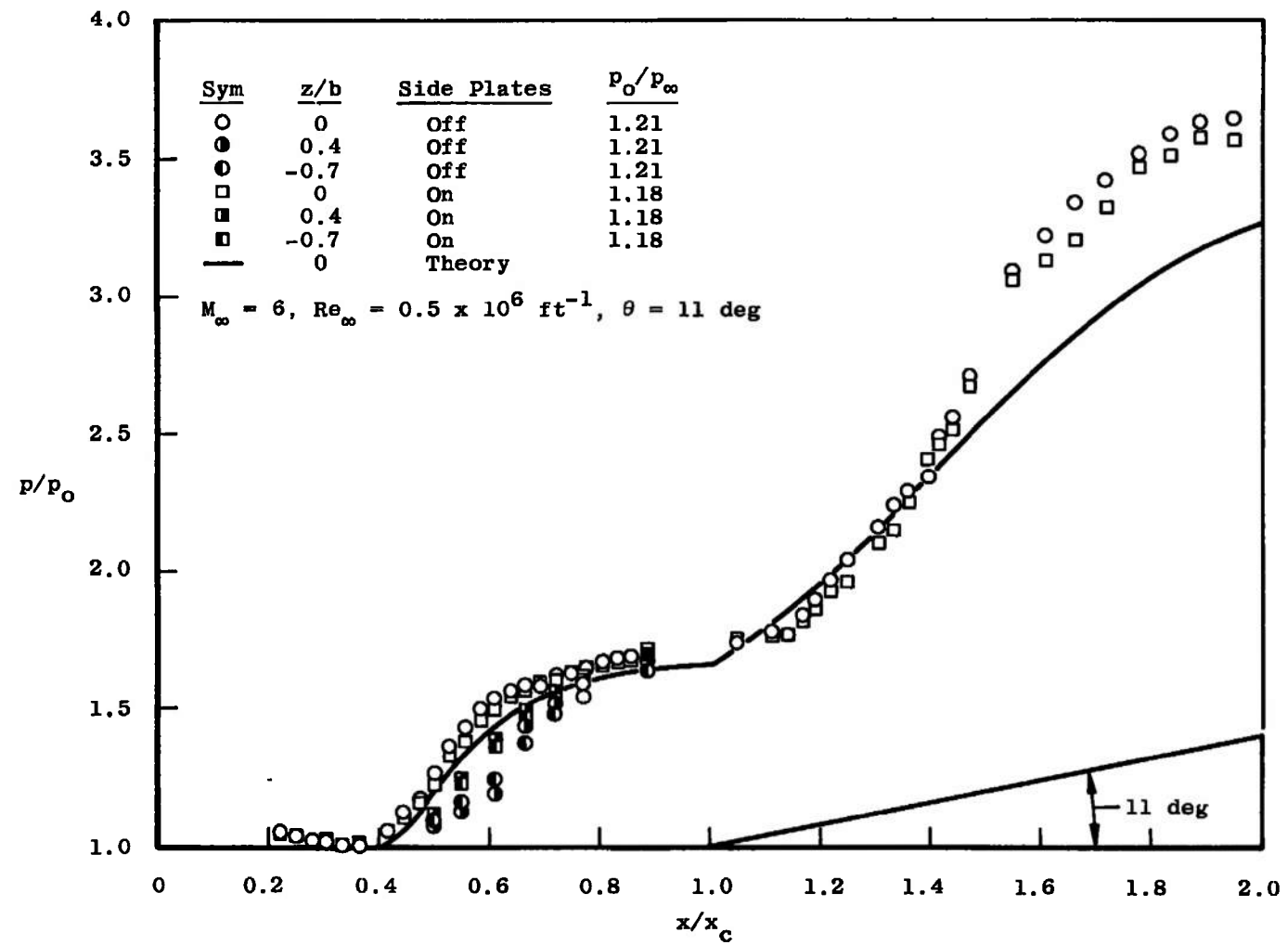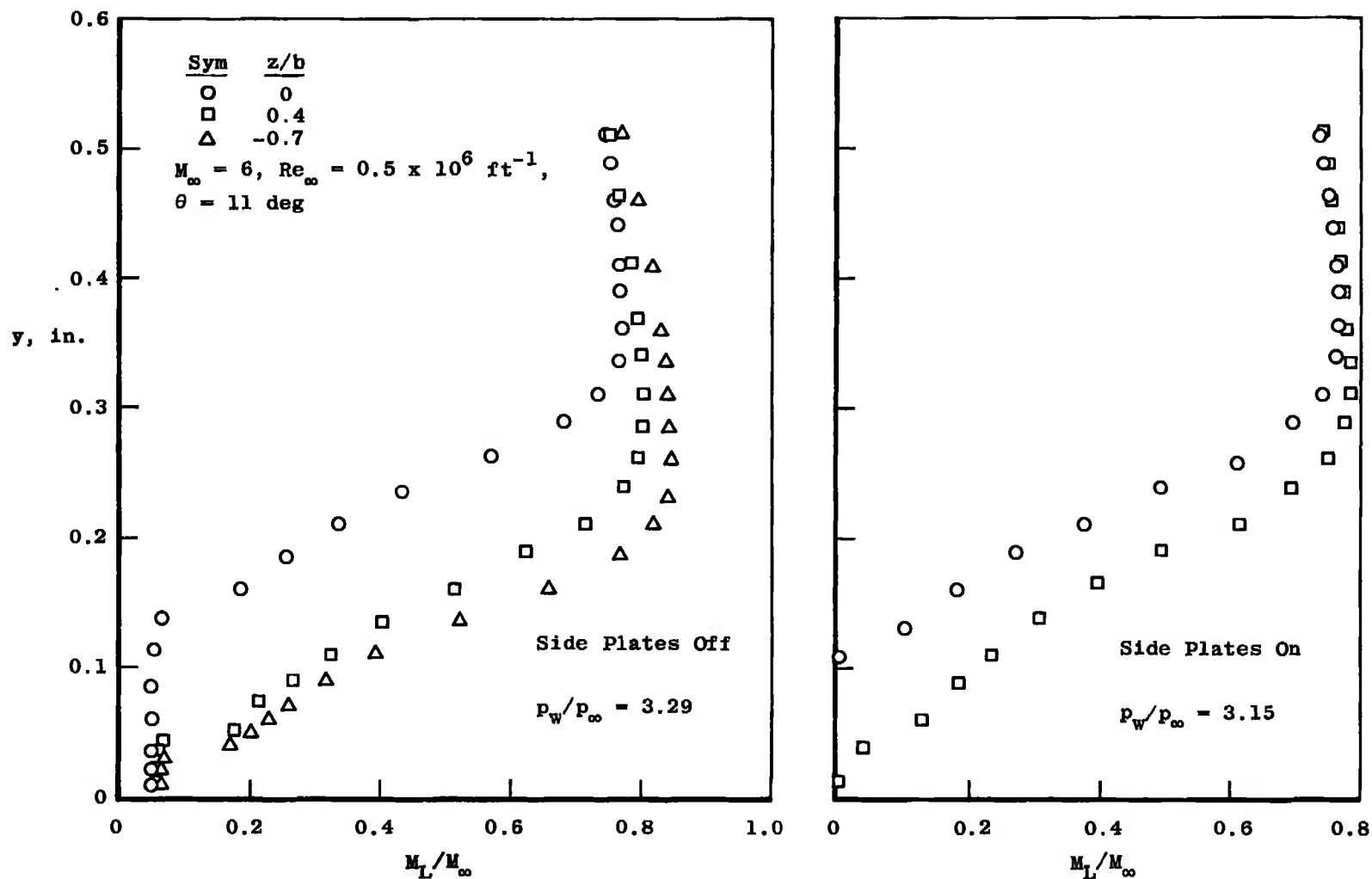
a. Chordwise Pressure Distribution

Fig. 4 Two-Dimensionality of Flow at $M_{w_1} = M_\infty = 6$, $Re_{x_c} = 0.38 \times 10^6$
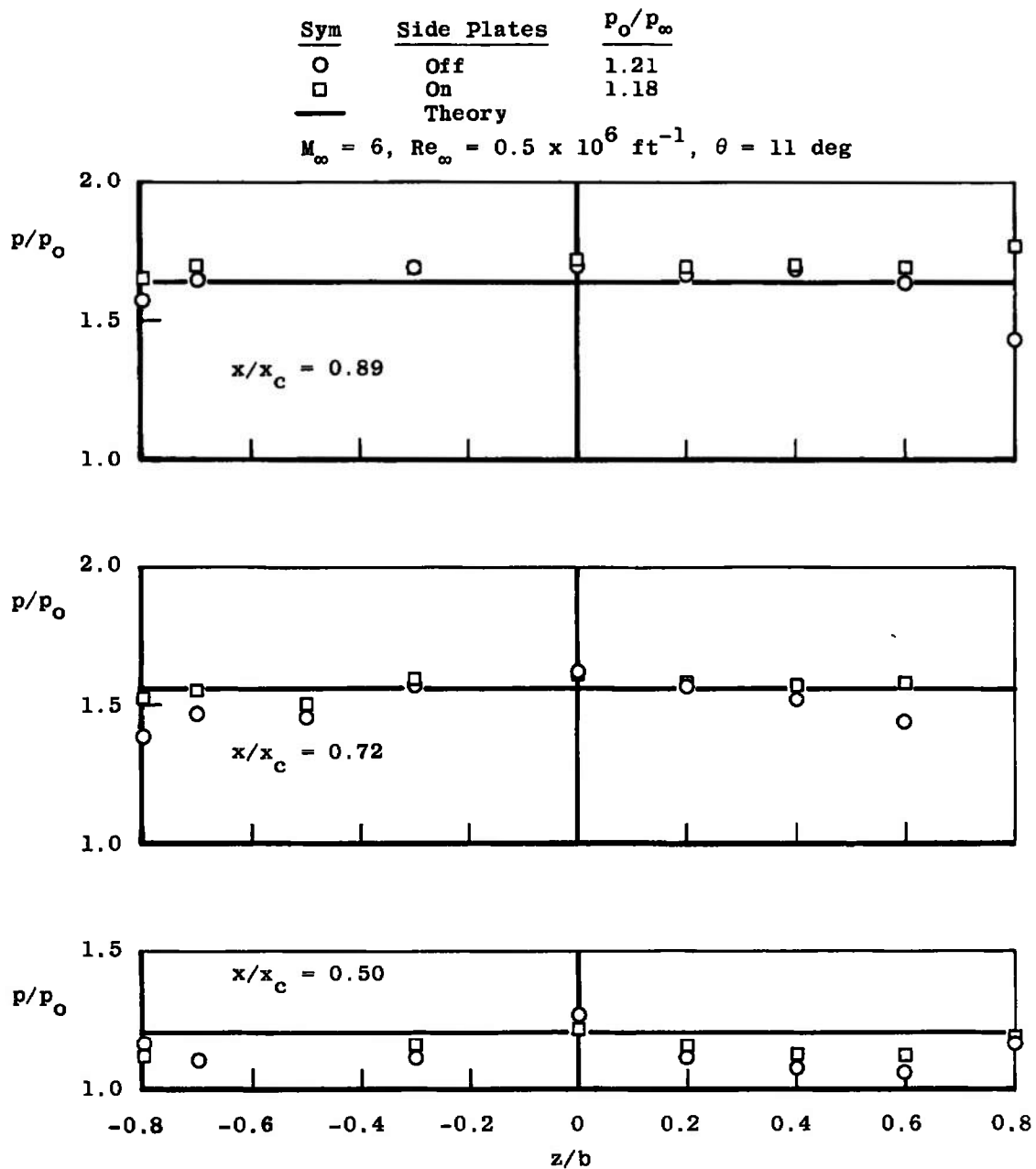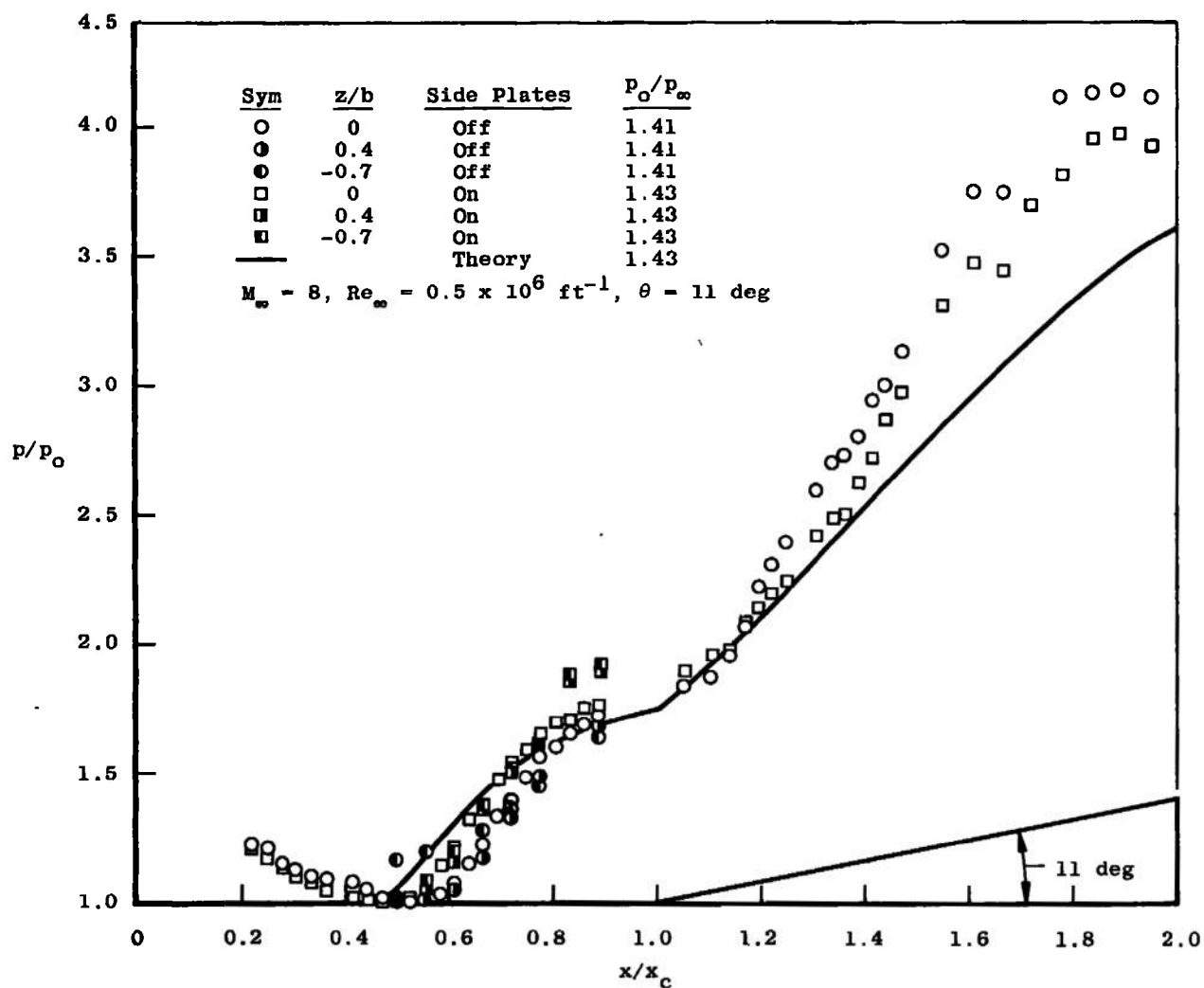
b. Spanwise Pressure Distribution

Fig. 4 Continued

c. Mach Number Profiles at x/x_c = 1.47
Fig. 4 Concluded

a. Chordwise Pressure Distribution

Fig. 5 Two-Dimensionality of Flow at $M_{w_I} \doteq M_\infty = 8$, $Re_{x_c} = 0.38 \times 10^6$

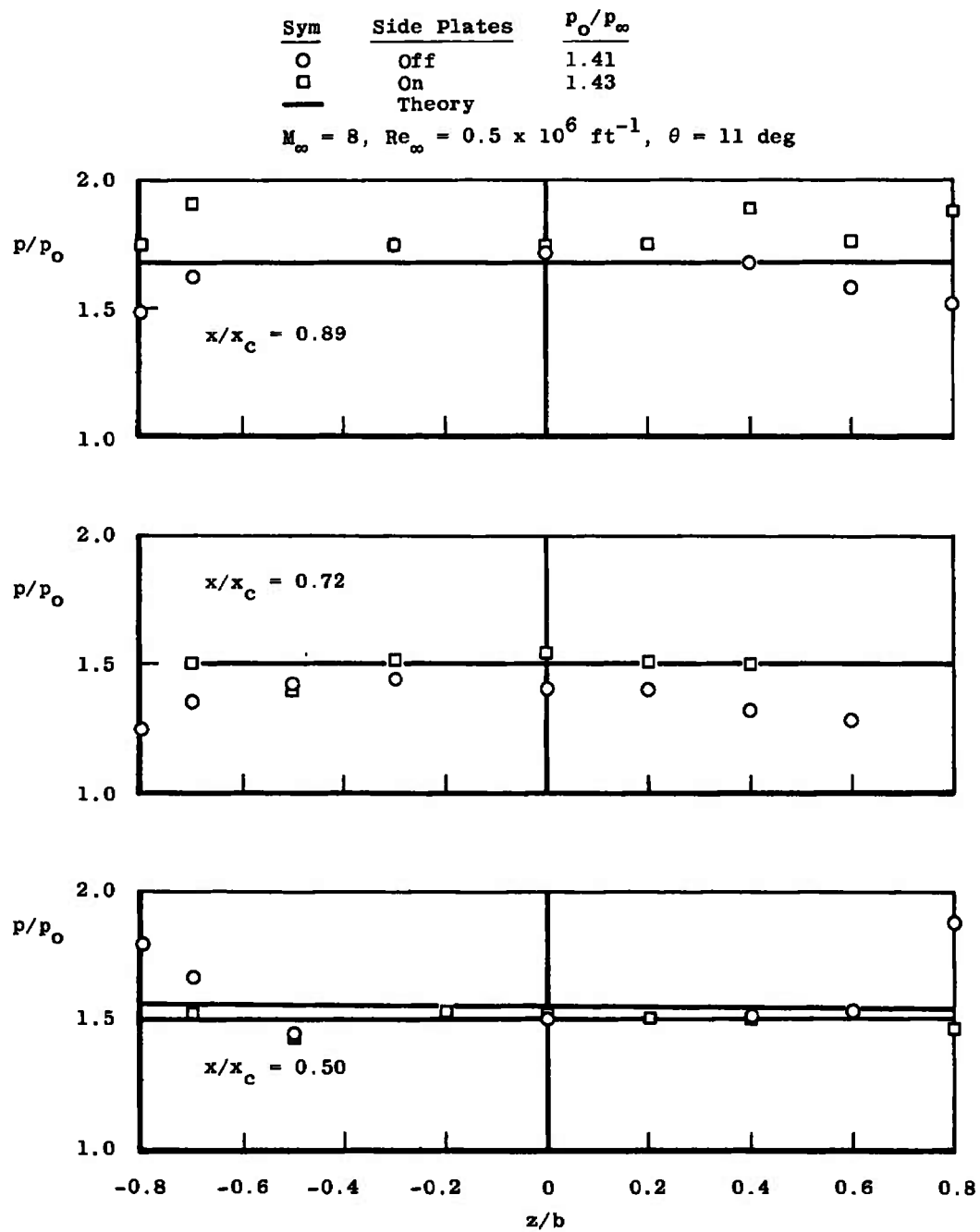b. Spanwise Pressure Distribution

Fig. 5 Continued

14

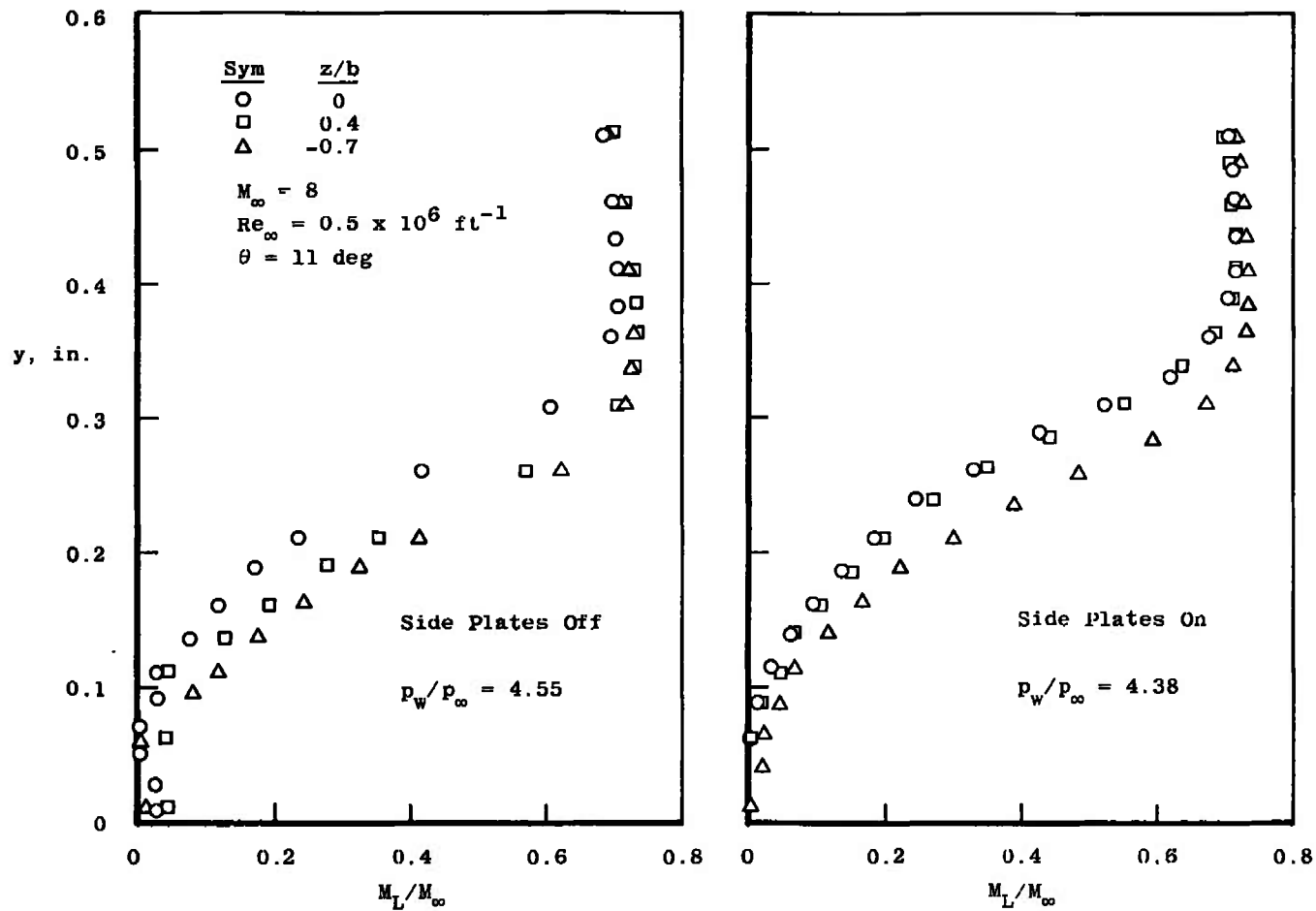c. Mach Number Profiles at x/x_c 1.47
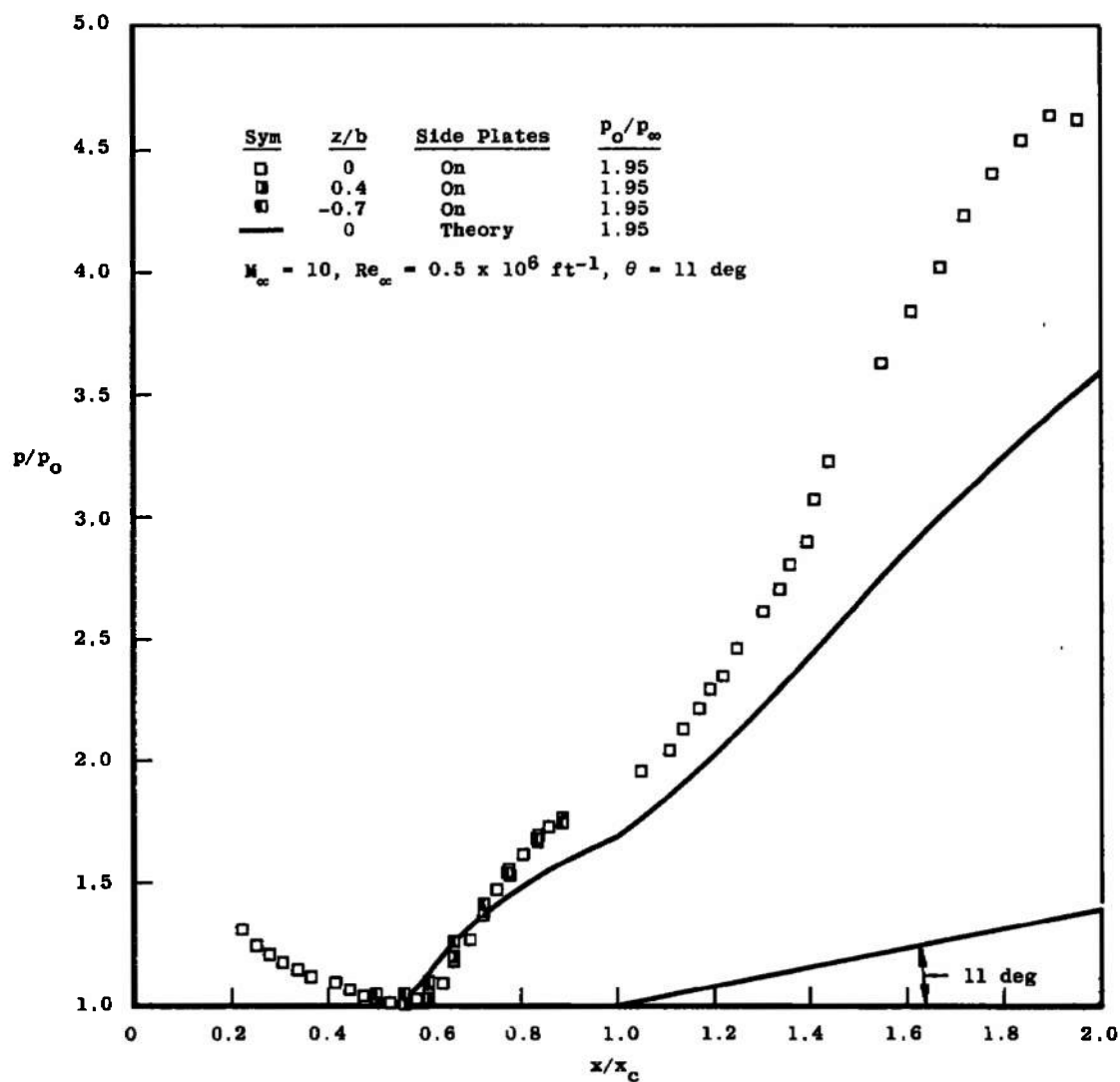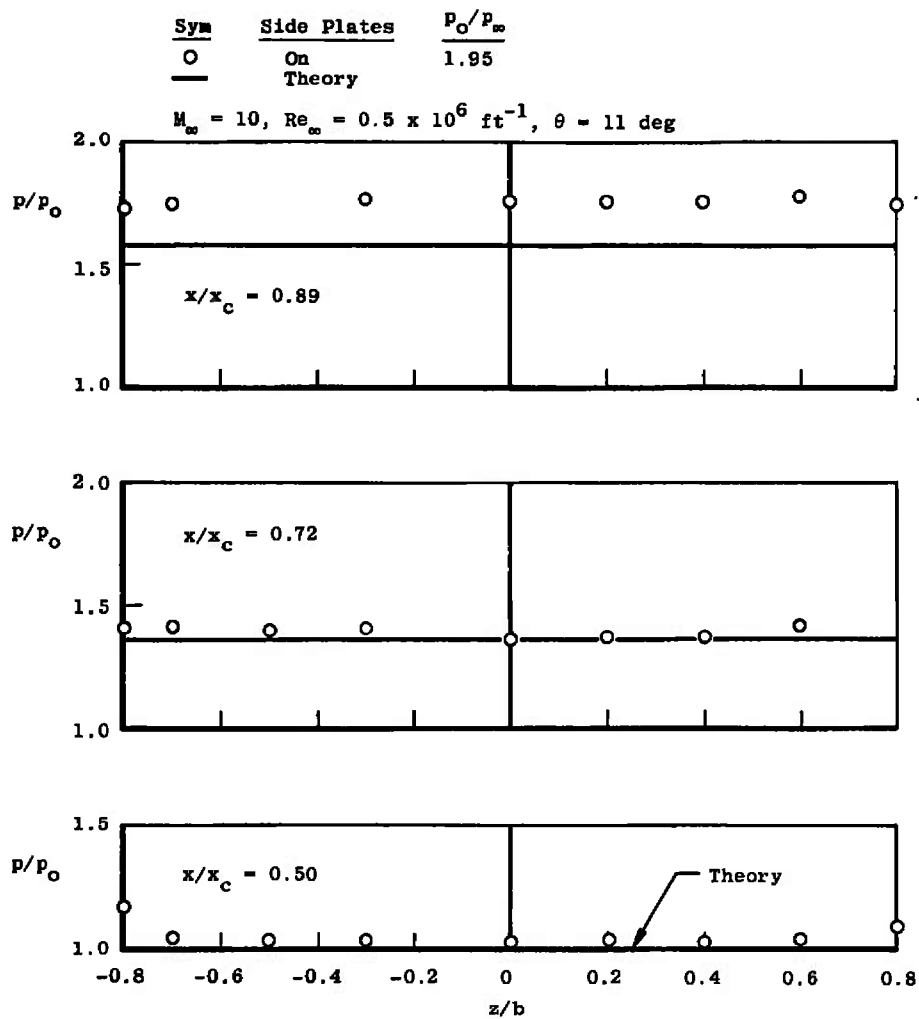
Fig. 5 Concluded

a. Chordwise Pressure Distribution

Fig. 6 Two-Dimensionality of Flow at $M_{w_1} = M_\infty = 10$, $Re_{x_c} = 0.38 \times 10^6$

16

b. Spanwise Pressure Distribution
Fig. 6 Concluded

The spanwise pressure distributions for M_{w_i} = 8 (Figs. 5a and b) show better agreement over a wider span, with the side paltes on, than the M_{w_i} = 6 data. When the side plates were removed, the relatively good agreement with theory for the flat-plate portion became worse, and the spanwise variations were amplified. The Mach number profiles (Fig. 5c) also indicate that the flow was more nearly the same for a wider span with the side plates on than with them removed. Therefore, because of the closer agreement with theory and the improved spanwise uniformity, the data with side plates on are considered to be more nearly two-dimensional.
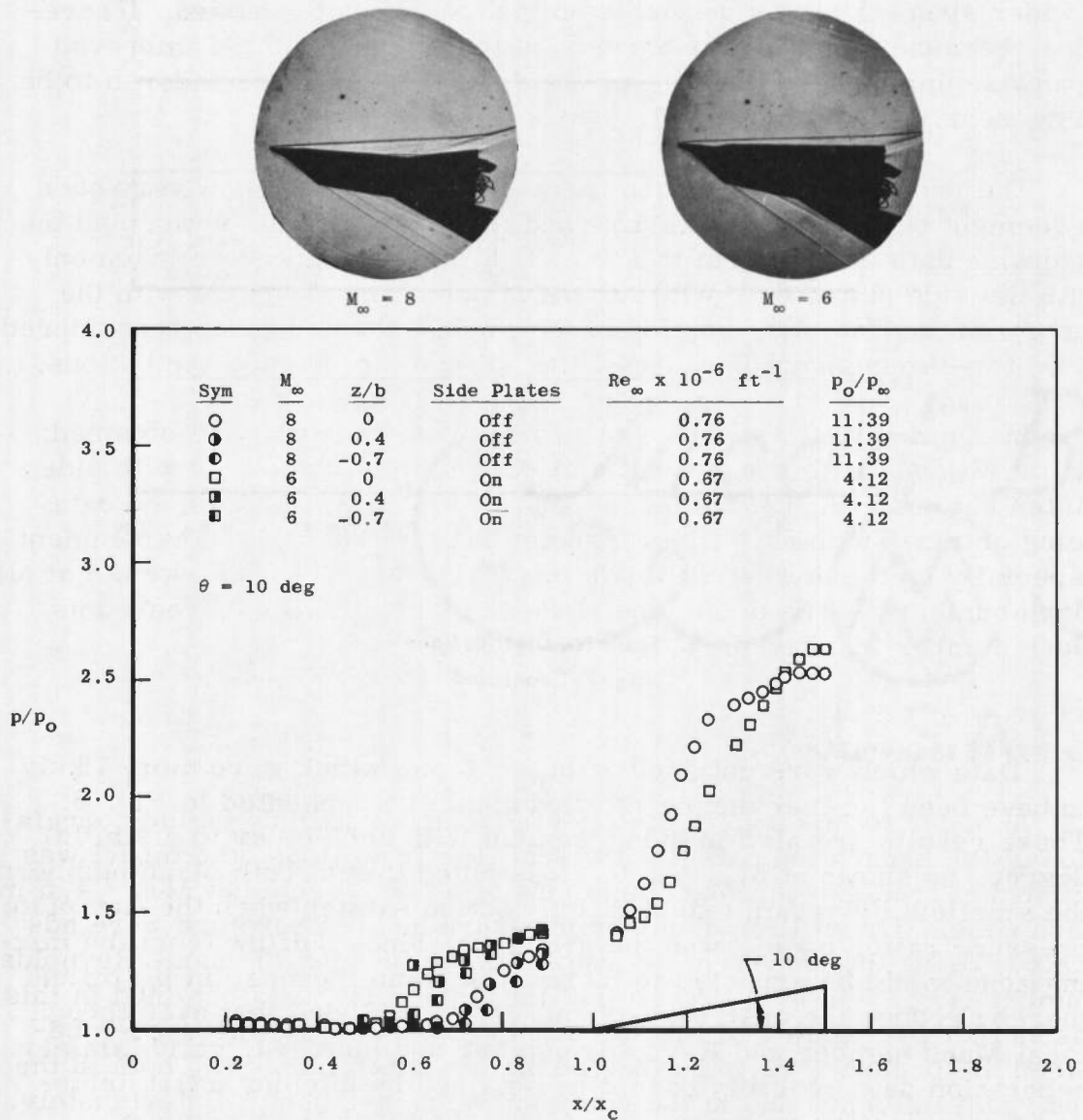
The pressure distributions for M_{w_i} = 10 (Fig. 6) show very good agreement between the centerline and the off-centerline rows, and the spanwise data are uniform to $z/b \le \pm0.6$. These data were taken only with the side plates on. While there is some disagreement with the theory on the flat-plate portion of the model, these data are considered to be two-dimensional because of the uniform spanwise distributions.

In summary, it appears that two-dimensional flow was obtained: (1) at M_{w_i} = 6 with and without side plates, (2) at M_{w_i} = 8 with side plates but not without, and (3) at M_{w_i} = 10 with side plates, no data being obtained without. Discrepancies between theory and experiment, especially on the downstream portion of the ramp, were observed at all Mach numbers. The magnitude of these discrepancies increased as Mach number increased.
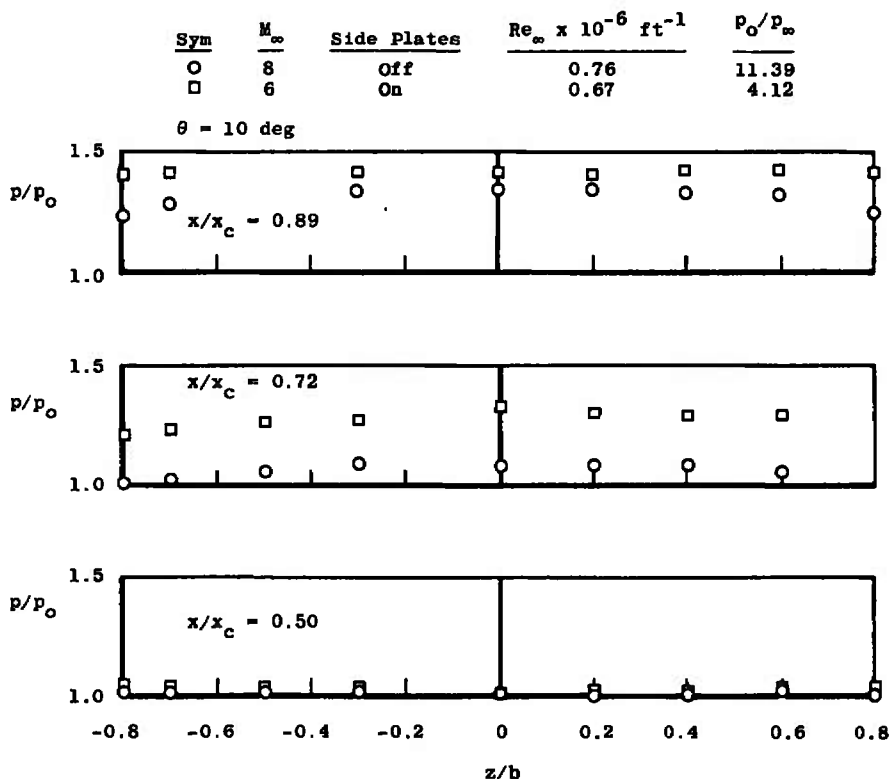
4.2 EFFECTS OF PITCH

In order to investigate the effects of model attitude on the correlation of the separation extent with local flow conditions, the model was pitched at free-stream Mach numbers of 6 and 8 such that M_{w_i} = 4.5 in each case. The stilling chamber pressure and temperature were adjusted, using the curves in the Appendix, to provide the same Reynolds number (Re_{x_c} = 0.75 x 10^6) on the flat plate. The data obtained in this manner are presented in Fig. 7, and they show large differences between the pressure distributions at the two Mach numbers, both in the upstream influence and in the ramp pressure gradient. Unfortunately, no data were obtained in a pitched attitude both with and without end plates at the same local conditions. The data at M_∞ = 6 were obtained with the side plates on; however, data at a lower Reynolds number (but at α_m = 0) as well as at a higher Reynolds number with the model pitched, indicated that there was little change when the side plates were removed. The data at M_∞ = 8 for z/b = 0.4 agree with the centerline data, and the spanwise distributions are uniform for a large span;

therefore, these data are considered to be two-dimensional. The shadowgraphs at $M_\infty = 8$ show that the boundary layer was, at least, transitional during reattachment. Because of the side plates, the state of the boundary layer was indeterminate at $M_\infty = 6$.

$M_\infty = 8$ $M_\infty = 6$

Sym	M_∞	z/b	Side Plates	$Re_\infty \times 10^{-6}$ ft^{-1}	p_o/p_∞
○	8	0	Off	0.76	11.39
◑	8	0.4	Off	0.76	11.39
◐	8	-0.7	Off	0.76	11.39
□	6	0	On	0.67	4.12
◼	6	0.4	On	0.67	4.12
◨	6	-0.7	On	0.67	4.12

$\theta = 10$ deg

10 deg

a. Chordwise Distributions

Fig. 7 Model Pitch Effect on Pressure Distribution at $M_{w_1} = 4.5$, $Re_{x_c} = 0.75 \times 10^6$

Sym	M_∞	Side Plates	$Re_\infty \times 10^{-6}$ ft^{-1}	p_o/p_∞
O	8	Off	0.76	11.39
□	6	On	0.67	4.12

$\theta = 10$ deg

b. Spanwise Distributions

Fig. 7 Concluded

Data which were obtained at $M_{W_j} = 6$ and which were more likely to have been laminar during reattachment are presented in Fig. 8. These results are also in disagreement with each other to a similar degree, as shown at $M_{W_j} = 4.5$. It is noted that at both Mach numbers the smallest upstream extent of interaction existed when the flat-plate pressure ratio, p_o/p_∞, was the greatest. Since outflow from the mixing zone would be expected to increase with an increase in p_o/p_∞ and thereby reduce the upstream extent, it is concluded that even though local Mach number and Reynolds number are matched, valid laminar separation data probably cannot be obtained by pitching a flat-plate-ramp combination to lower appreciably the local Mach number.
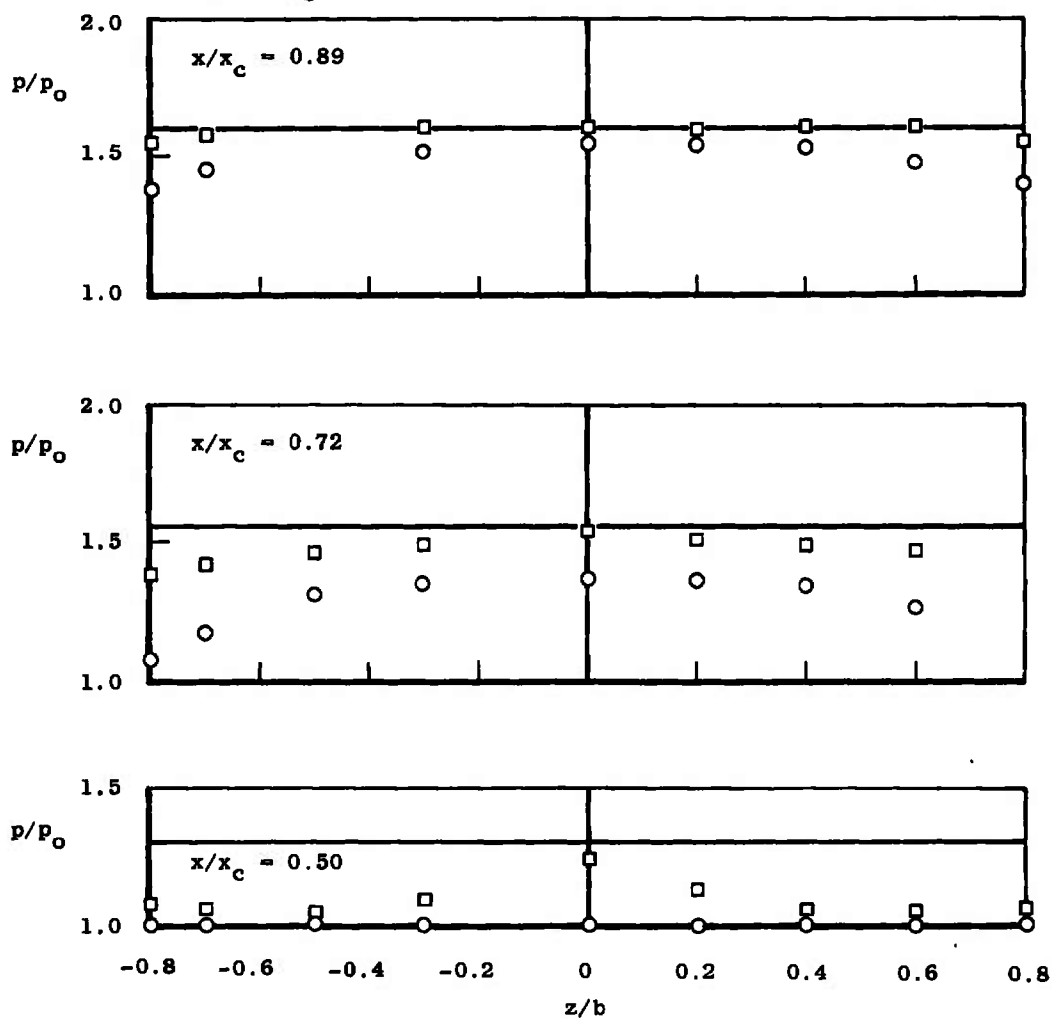
$M_\infty = 8$ $M_\infty = 6$

Sym	M_∞	z/b	Side Plates	$Re_\infty \times 10^{-6}$ ft^{-1}	p_O/p_∞
◯	8	0	Off	0.65	5.02
◑	8	0.4	Off	0.65	5.02
◖	8	-0.7	Off	0.65	5.02
☐	6	0	Off	1.0	1.12
◪	6	0.4	Off	1.0	1.12
◧	6	-0.7	Off	1.0	1.12
——	6	0	Theory	1.0	1.12
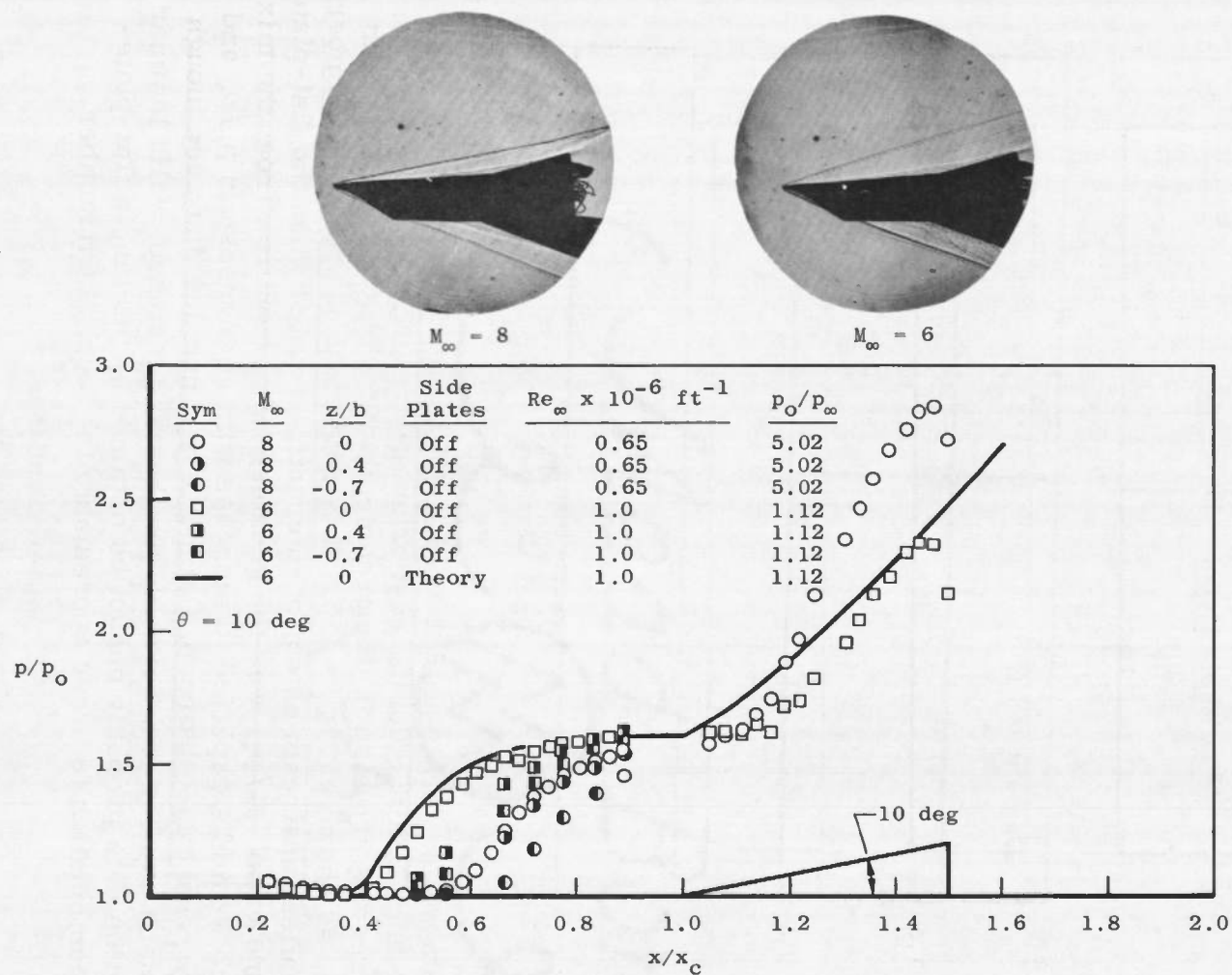
$\theta = 10$ deg

-10 deg

a. Chordwise Distribution

Fig. 8 Model Pitch Effect on Pressure Distribution at $M_{w_1} = 6$, $Re_{x_c} = 0.75 \times 10^6$

21

| Sym	M_∞	Side Plates	Re_∞ x 10^{-6} ft^{-1}	p_0/p_∞
O	8	Off	0.65	5.02
□	6	Off	1.0	1.12
——	6	Theory	1.0	

$\theta = 10$ deg

b. Spanwise Distribution
Fig. 8 Concluded

4.3 EXTENT OF LAMINAR FLOW

The data presented in Fig. 9 were used to judge if the boundary layer was laminar through reattachment at $M_\infty = M_{w_i} = 6$. As seen in Figs. 9a and b, the beginning of the interaction region moved upstream as Reynolds number increased; however, the rate of change was less than indicated by the theory. It has been shown (Refs. 2, 6, 7, and 8) that the extent of upstream influence should increase as Reynolds number is increased if the boundary layer is laminar through reattachment. While none of the flat-plate centerline pressure distributions (Fig. 9a) agree exactly with the theory of Lees and Reeves, Ref. 5 as modified in Ref. 4, the lowest Reynolds number data are the closest. For comparison to the present data on the ramp, data from Ref. 6 are presented in Fig. 9a for a slightly different ramp angle and a lower Reynolds number. These data on the ramp show good agreement with the theory, although the upstream interaction extent (also shown in Fig. 9b) is somewhat less than predicted. Data from Ko and Kubota (Ref. 7) are shown in Fig. 9b to have relatively good agreement with the theory.
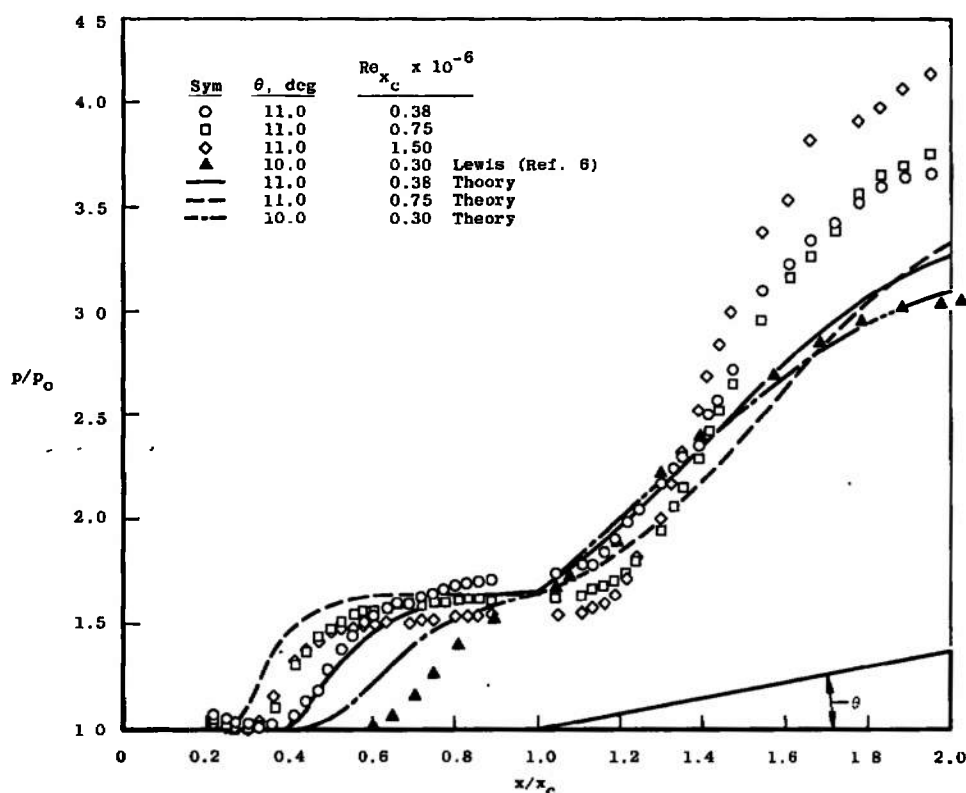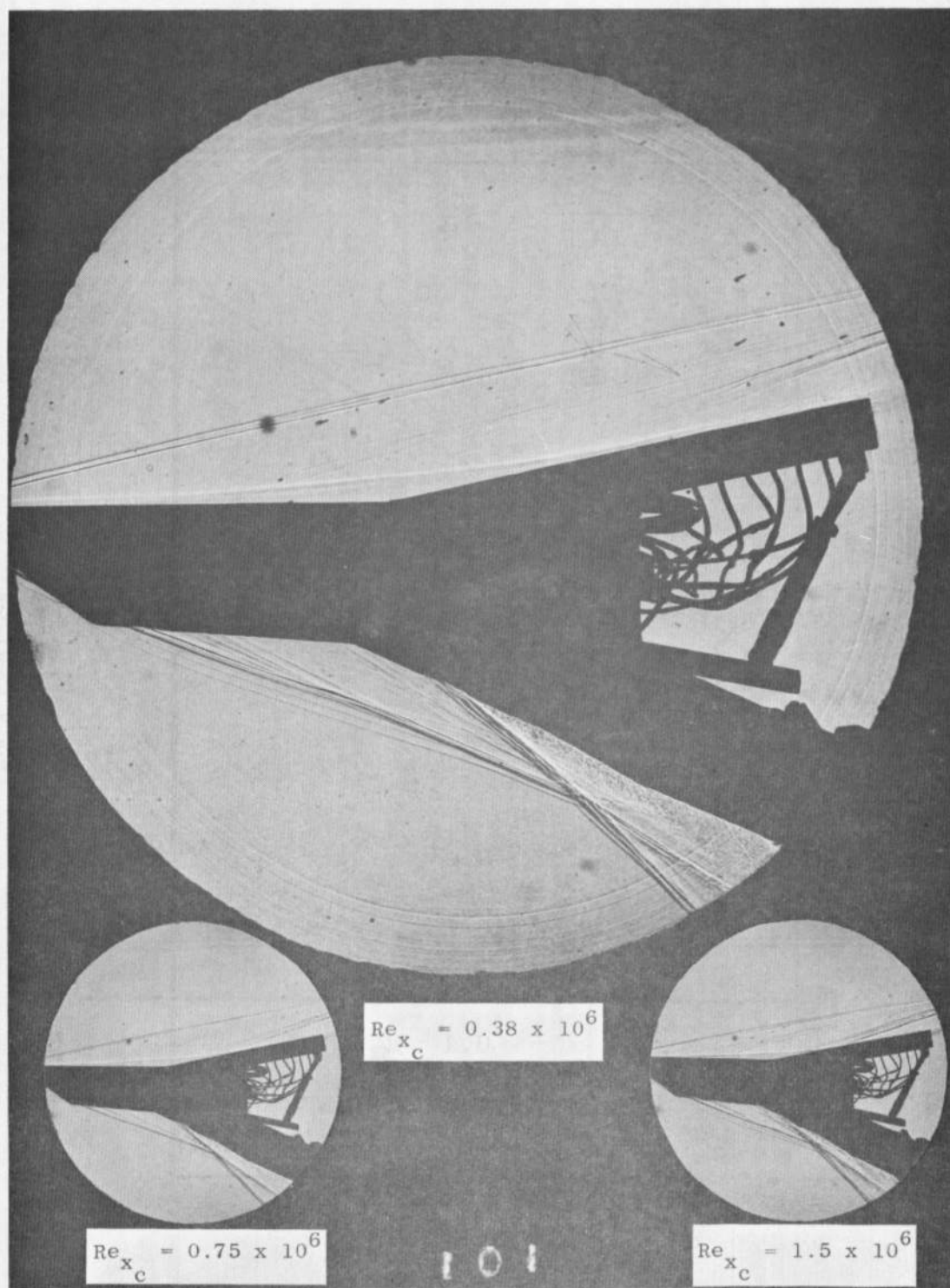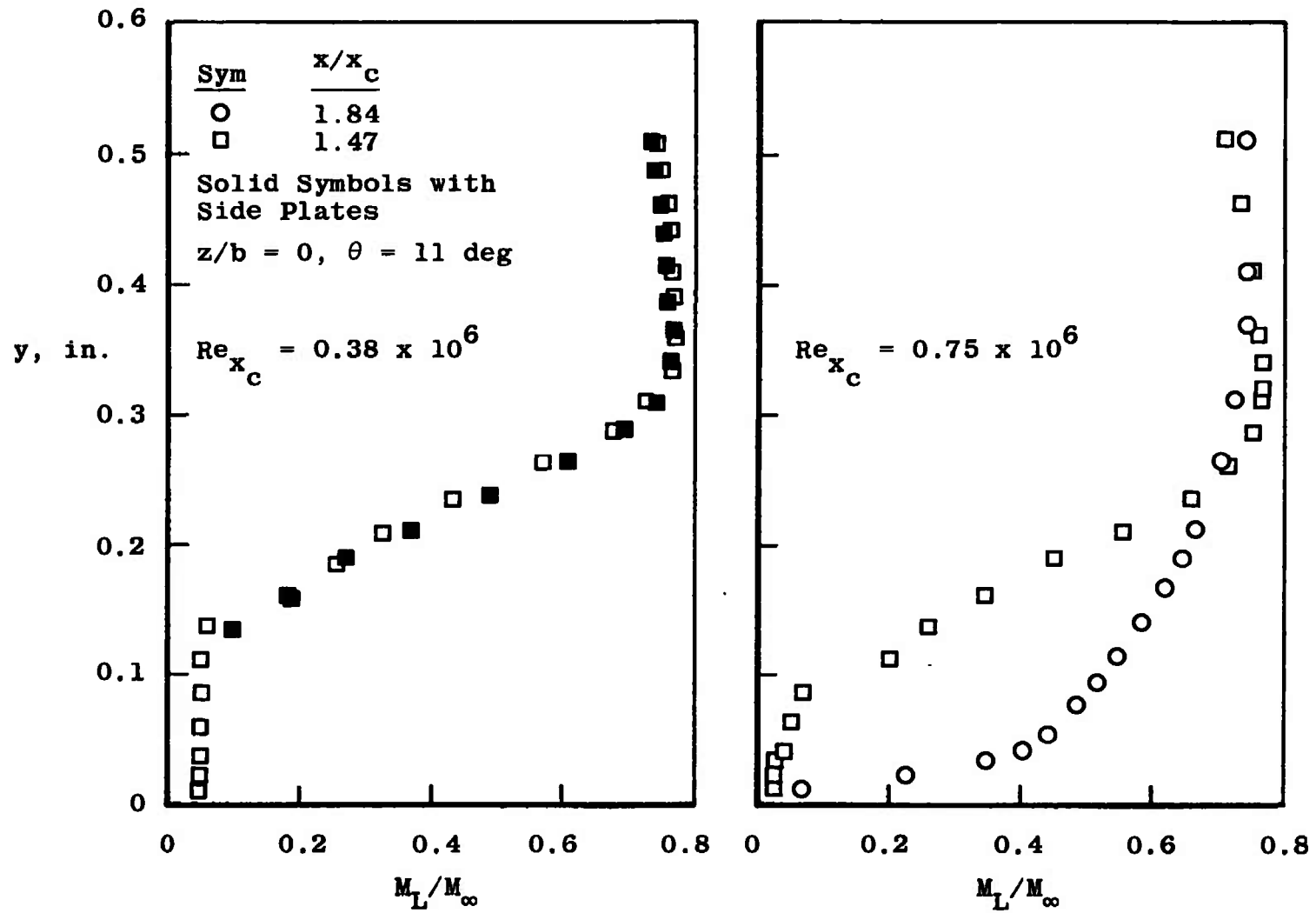

a. Centerline Pressure Distribution

Fig. 9 Effect of Reynolds Number Change at $M_{w_1} = M_\infty = 6$
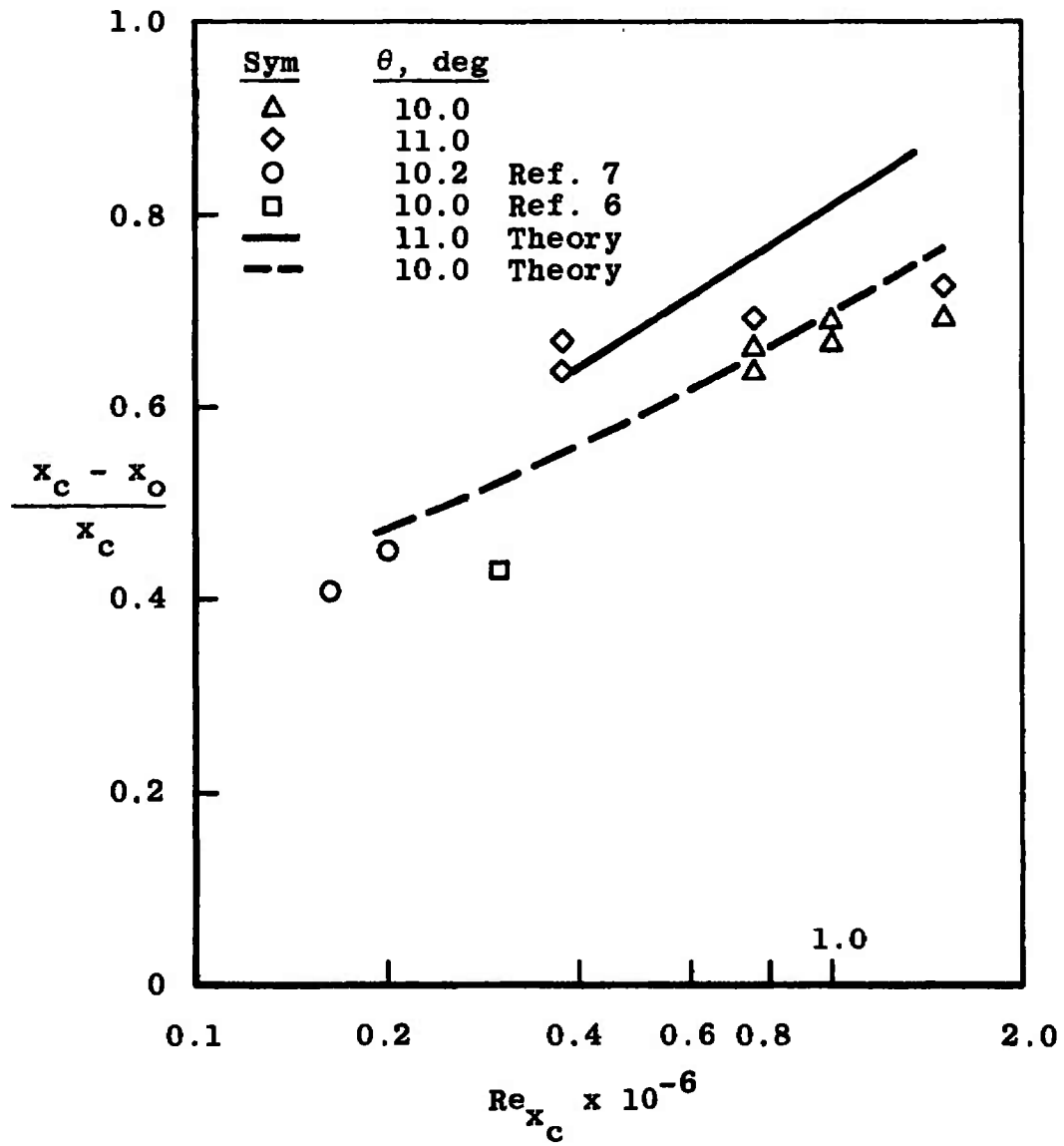
b. Change in Interaction Length
Fig. 9 Continued

Re$_{x_c}$ = 0.38 x 10^6

Re$_{x_c}$ = 0.75 x 10^6

Re$_{x_c}$ = 1.5 x 10^6

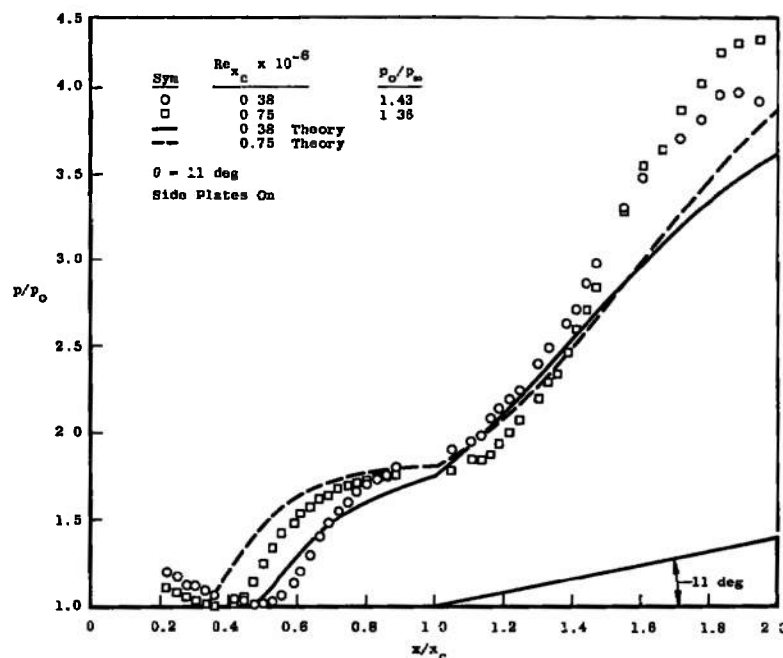c. Shadowgraphs at θ = 11 deg
Fig. 9 Continued

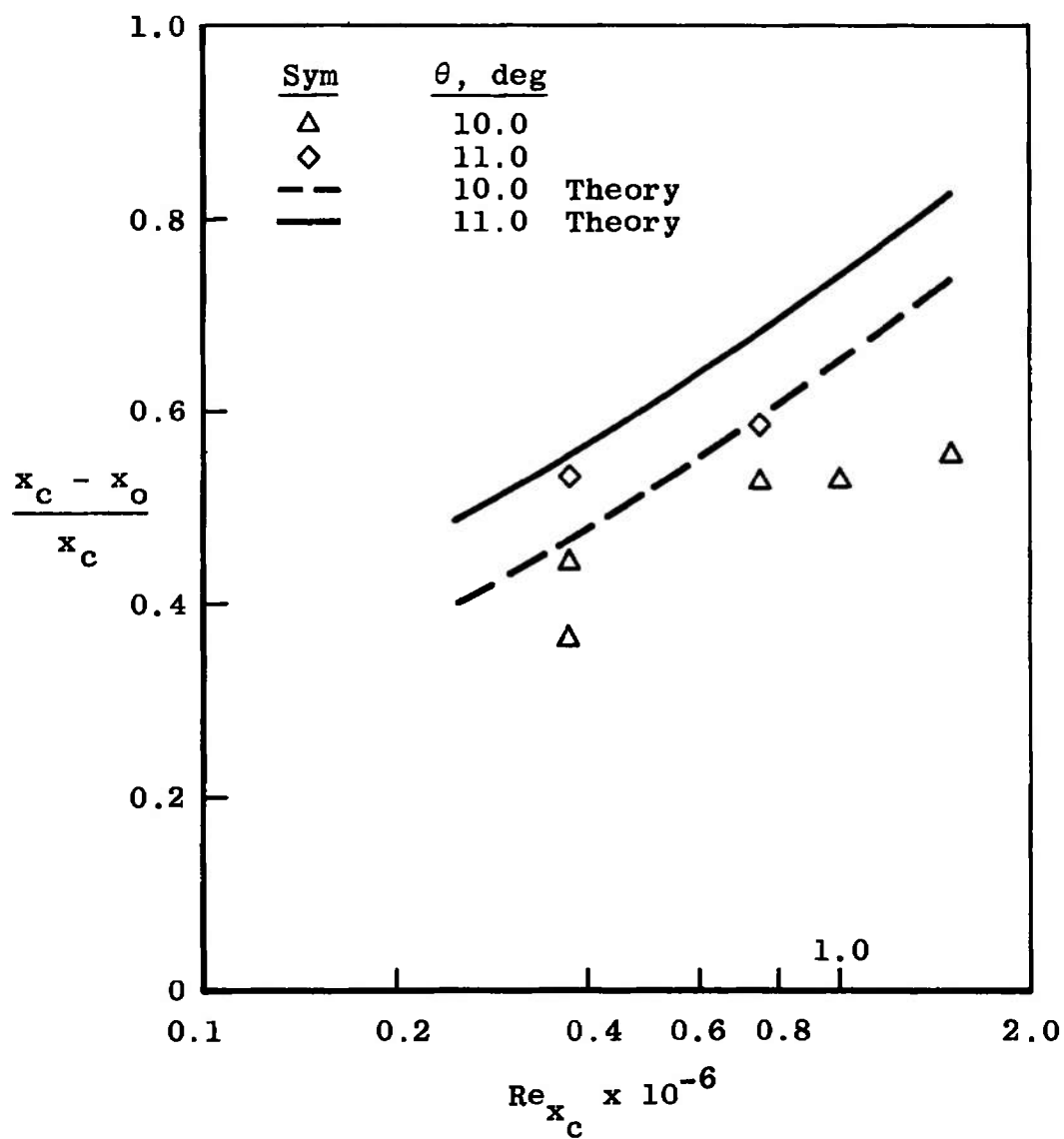d. Mach Number Profiles

Fig. 9 Concluded

The shadowgraph pictures (Fig. 9c) indicate that the boundary layer was laminar through reattachment for the lowest Reynolds number and, at least, transitional for the higher Reynolds numbers. Mach number profiles on the ramp for two locations are presented in Fig. 9d and show that the recirculation region was smaller at higher Reynolds number, i.e., reattachment occurred earlier. This also indicates that the boundary layer was at least transitional at reattachment for the higher Reynolds numbers. As stated before, the choice of static pressure used for data reduction was the reason that some of the curves do not go to a Mach number ratio of zero in the recirculation region.

The pressure data for M_{w_i} = 8 and 10 were taken with the side plates installed, and shadowgraphs were obtained with them removed at only the lowest Reynolds number. The data (Figs. 10 and 11) show the same general trends as for M_{w_i} = 6. Only the lowest Reynolds number at M_{w_i} = 8 was judged to be laminar through reattachment. This is true for both ramp angles tested, as indicated in Fig. 10b. The M_{w_i} = 10 data (Fig. 11) indicate, as based on the variation of the upstream extent with Reynolds number increase, that the reattaching boundary layer was laminar for all ramp angles for the two lowest Reynolds numbers and probably for the highest (Re_{x_c} = 0.75 x 10^6). The reattachment pressure distribution is, as in all previous data, very different from the theory.
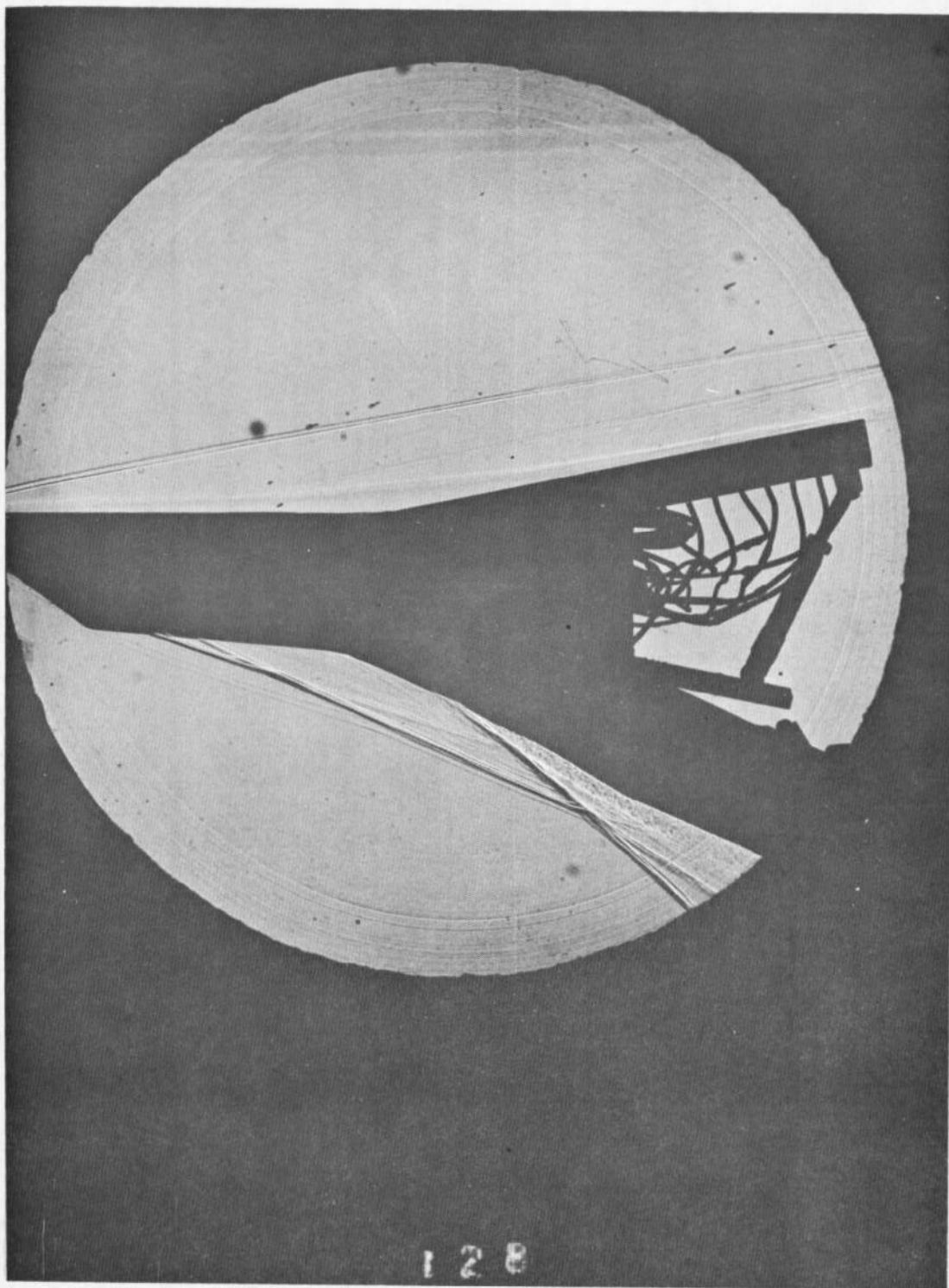

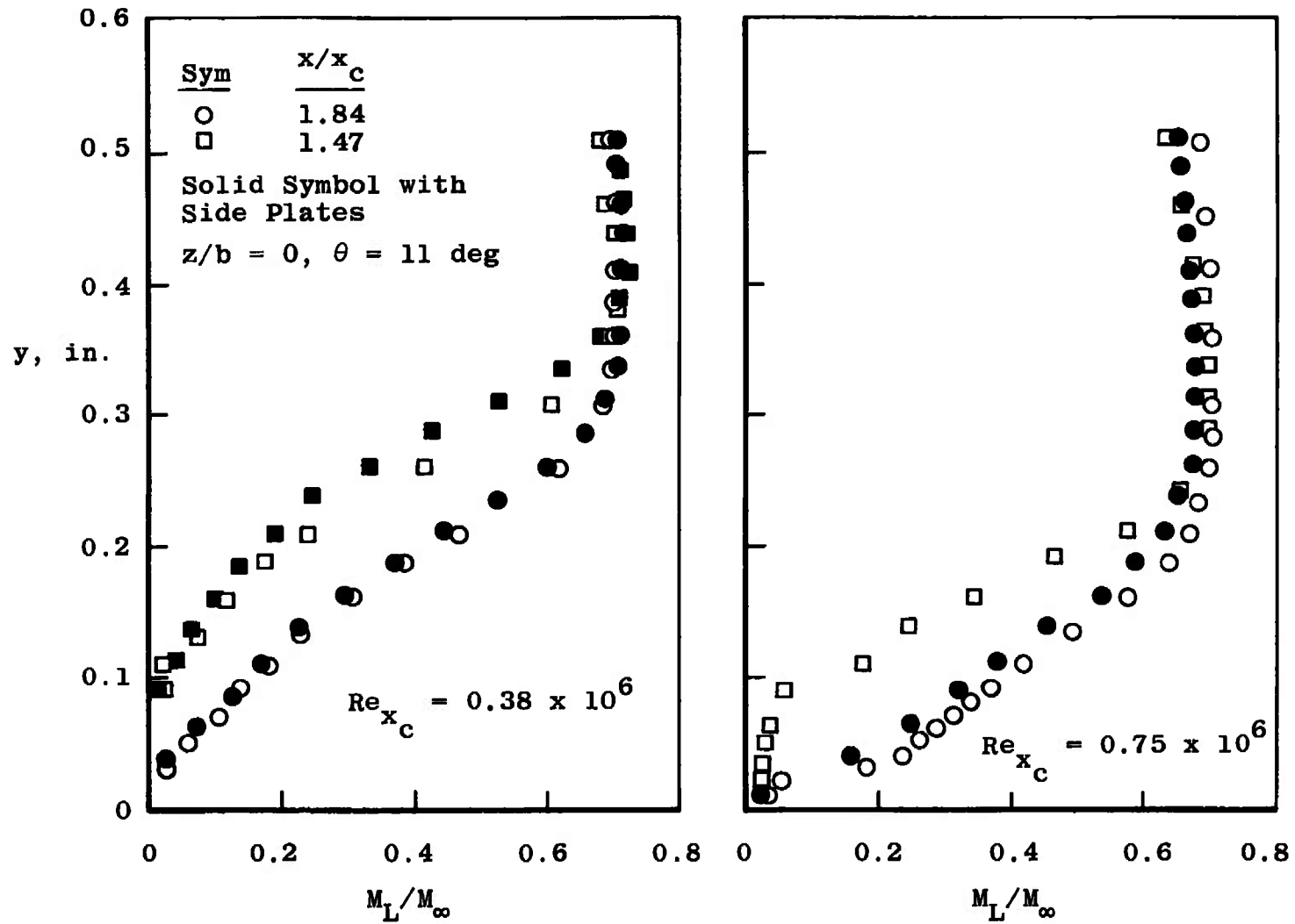a. Centerline Pressure Distribution

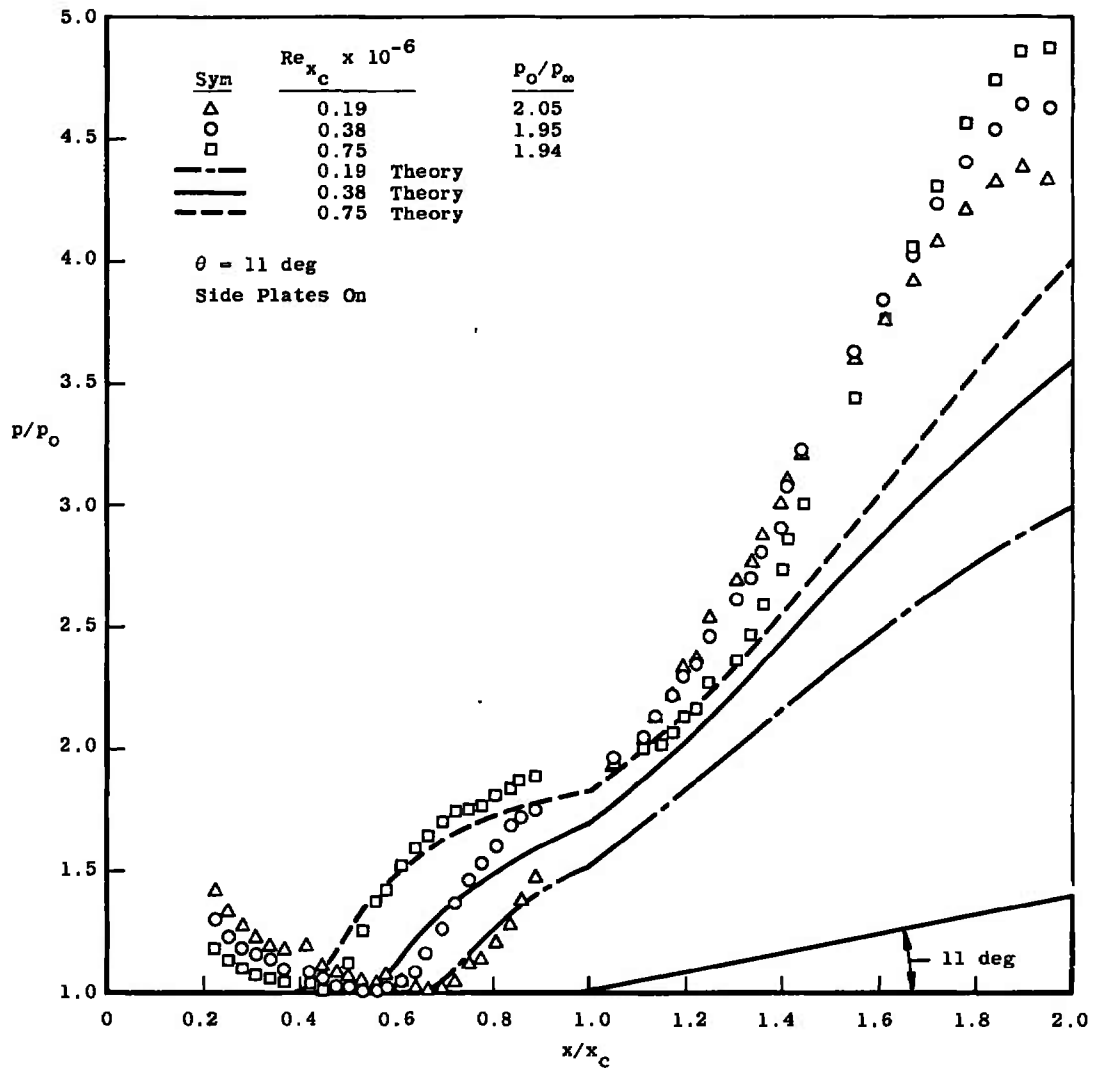Fig. 10 Effect of Reynolds Number Change at $M_{w_1} = M_\infty = 8$

b. Change in Interaction Length

Fig. 10 Continued

c. Shadowgraph at $Re_{x_c} = 0.38 \times 10^6$, $\theta = 11$ deg
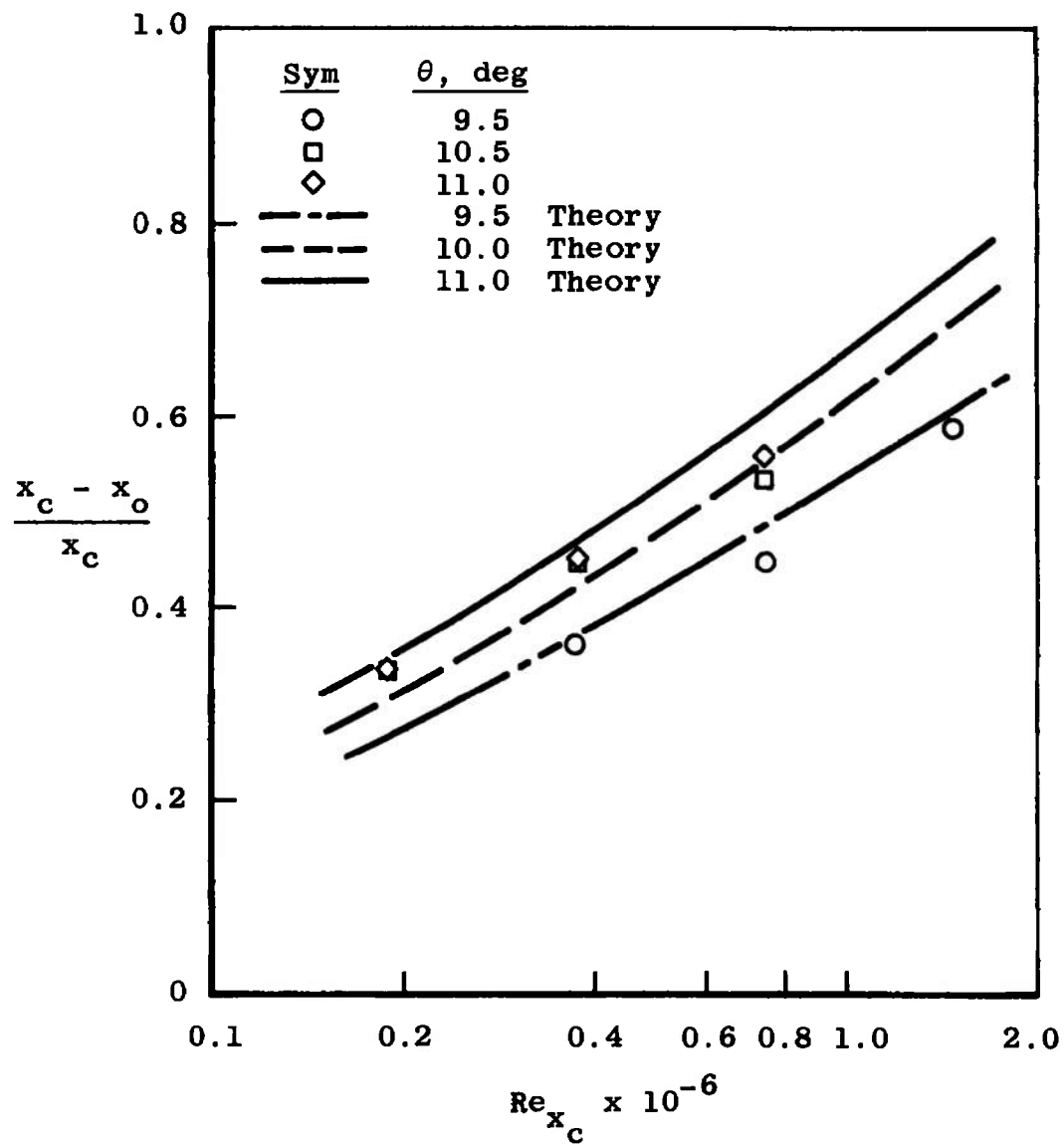Fig. 10 Continued
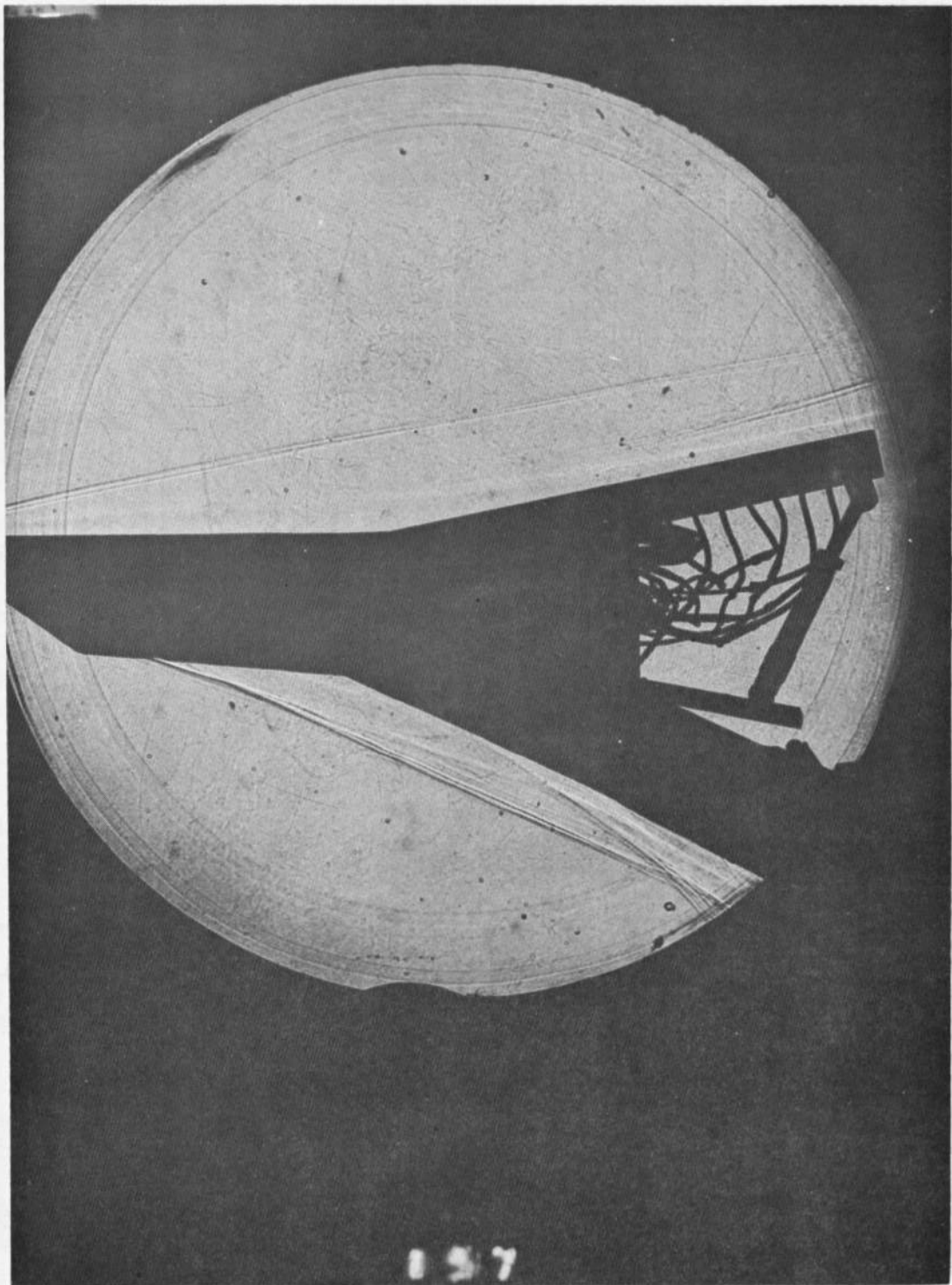
29

d. Mach Number Profiles
Fig. 10 Concluded

a. Centerline Pressure Distribution

Fig. 11 Effect of Reynolds Number Change at $M_{w_1} = M_\infty = 10$

b. Change in Interaction Length

Fig. 11 Continued

c. Shadowgraph at $Re_{x_c} = 0.19 \times 10^6$, $\theta = 11$ deg
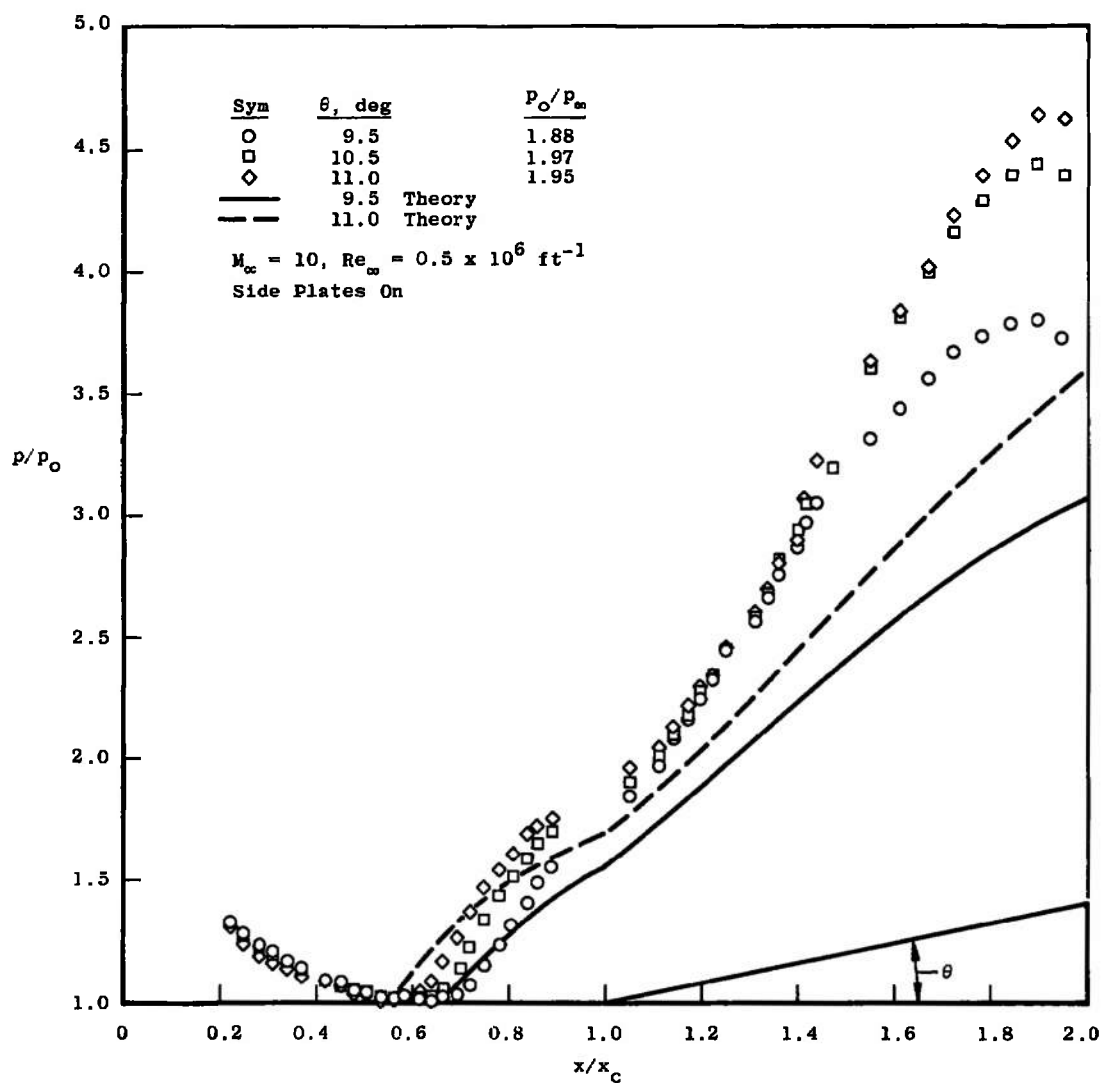Fig. 11 Concluded

4.4 REATTACHMENT PRESSURE RISE

As pointed out in previous discussions, the pressure gradient on the ramp was in all cases larger than that predicted by theory. In general, this is considered to be an indication of nonlaminar reattachment. However, there appears to be enough evidence from the upstream extent data and the shadowgraphs to indicate that the reattaching boundary layer was laminar, at least at the lowest Reynolds number. The present data with the long ramp are considered to be free of geometry limitations because the theoretical reattachment point is well upstream of the trailing edge of the ramp. It remains, then, to determine the cause of this discrepancy. Other investigators have obtained data which in most cases, when the reattachment has been shown to be laminar, agree reasonably well with the theory of Lees and Reeves. The theory has not previously been extended to the higher Mach numbers of the present test. If, however, there were some fallacy in the theory at the higher Mach number, it would still leave the disagreement at Mach number 6 unexplained because other authors, Ref. 5 for instance, have obtained better agreement at this Mach number. It is, of course, pertinent to note that the theoretical results presented here are for the case of $S_w = 0$, which is relatively far removed from the actual test conditions investigated. Perhaps the most remarkable fact derived from the comparisons of theory and experiment is the general agreement found upstream of the ramp despite the significant differences observed on the ramp.

There is one major difference between the present work and that of Refs. 4, 6, 7, and 8. The maximum flat-plate length to the hinge line, x_c, of previous work was 5 in., whereas the present model was 9 in. Lewis (Ref. 6) found no change in either the upstream influence or the reattachment pressure rise for lengths of $x_c = 2$, 3, and 5 in. at constant Reynolds number. However, the aspect ratios, $x_c/2b$, for these lengths were 1.5, 1.33, and 0.8, respectively. The aspect ratio of the present model was 2.22, greater than that for even the shortest flat-plate length of Ref. 6. An investigation of the effects of flat-plate length and/or aspect ratio was planned for the present study and in fact was being started when the model failure occurred. It was felt that the pressure rise on the ramp may be a function of the flat-plate length even though the boundary layer remains laminar through reattachment. There is still the possibility, especially at $M_{w_i} = 6$, that transition at or even downstream of reattachment caused the unusual pressure rise on the ramp. Further work is needed to resolve these questions.

4.5 RAMP ANGLE EFFECT

As pointed out by other authors, Ref. 7 for instance, the extent of the upstream influence of the ramp is sensitive to small variations in angle of attack. Figure 12 shows a similar sensitivity to a small change in ramp angle. An increase of 1.5 deg in ramp angle at M_{w_i} = 10 caused a measurable increase in the extent of the upstream interaction and in particular the maximum pressure ratio obtained on the ramp. As in previous figures, this pressure rise was greater than that predicted by theory.

Sym	θ, deg	p_o/p_∞	
O	9.5	1.88	
□	10.5	1.97	
◇	11.0	1.95	
——	9.5	Theory	
– –	11.0	Theory	

M_∞ = 10, Re_∞ = 0.5 x 10^6 ft^{-1}

Side Plates On

a. Re_{x_c} = 0.38 x 10^6

Fig. 12 Effect of Ramp Angle Change on Centerline Pressure Distribution at M_{w_1} = M_∞ = 10
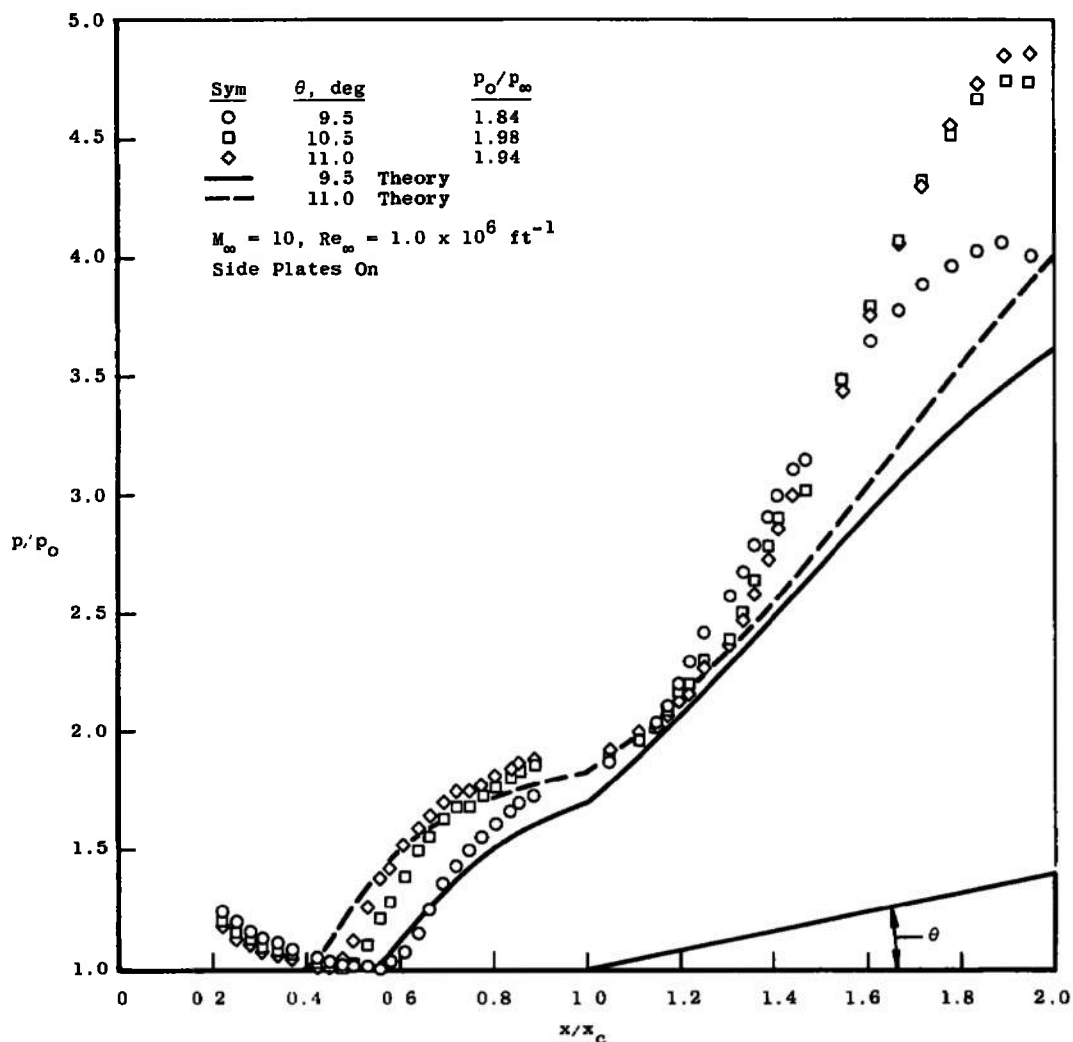
b. $Re_{x_c} = 0.75 \times 10^6$
Fig. 12 Concluded

4.6 INFLUENCE OF MASS BLEED

As stated in Section I, only a limited amount of data was obtained with the mass-removal slot open. These data were obtained before the extension was added to the ramp, and therefore, the reattachment was probably forced to occur further upstream than it would have with the long ramp (at least in the no-bleed case with the model pitched). Figure 13 shows that with the model pitched to obtain a local Mach number of 4.5, a bleed-slot inlet size of only 0.062 in. (area = 1.12 in.[2]) removed all of the separation. These data are, as indicated in the shadowgraphs, at least transitional during reattachment. The data obtained

for M_{w_i} = 6 (Fig. 14) show that the increase in upstream interaction (over that at M_{w_i} = 4.5, but at the same Re_{x_c}) required a larger slot inlet area in order to remove all of the separation. The upstream influence without bleed in Figs. 14a and b remained approximately the same when the Reynolds number was increased; therefore, these data are also considered to be transitional at reattachment. As in the case of the M_{w_i} = 4.5 data, when the separation was completely removed, a pressure ratio of less than 1.0 was obtained well upstream of the inlet to the bleed slot.
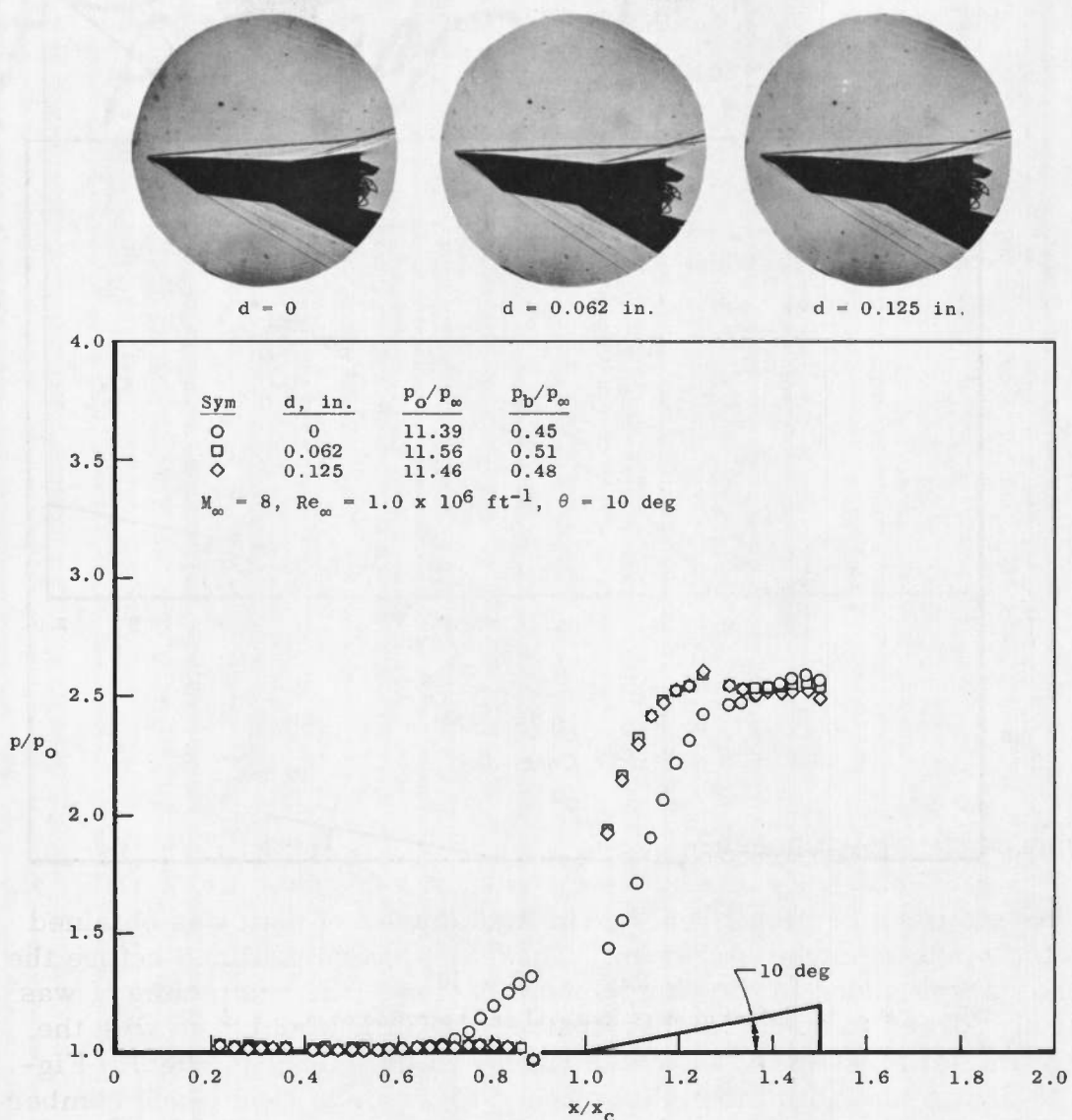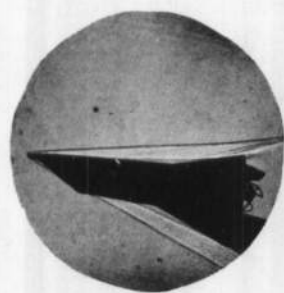

d = 0   d = 0.062 in.   d = 0.125 in.

Sym	d, in.	p_o/p_∞	p_b/p_∞
○	0	11.39	0.45
□	0.062	11.56	0.51
◇	0.125	11.46	0.48

M_∞ = 8, Re_∞ = 1.0 x 10^6 ft^{-1}, θ = 10 deg

Fig. 13 Effect of Mass Removal on Separation at M_{w_i} = 4.5, Re_{x_c} = 1.06 x 10^6

d = 0   d = 0.062 in.

Sym	d, in.	p_o/p_∞	p_b/p_∞
○	0	4.98	0.41
□	0.062	5.01	0.47

$M_\infty = 8$, $Re_\infty = 0.88 \times 10^6$ ft^{-1},

$\theta = 10$ deg

10 deg
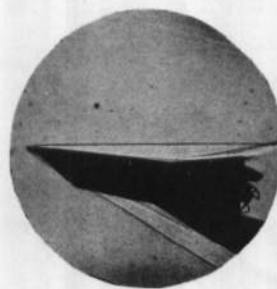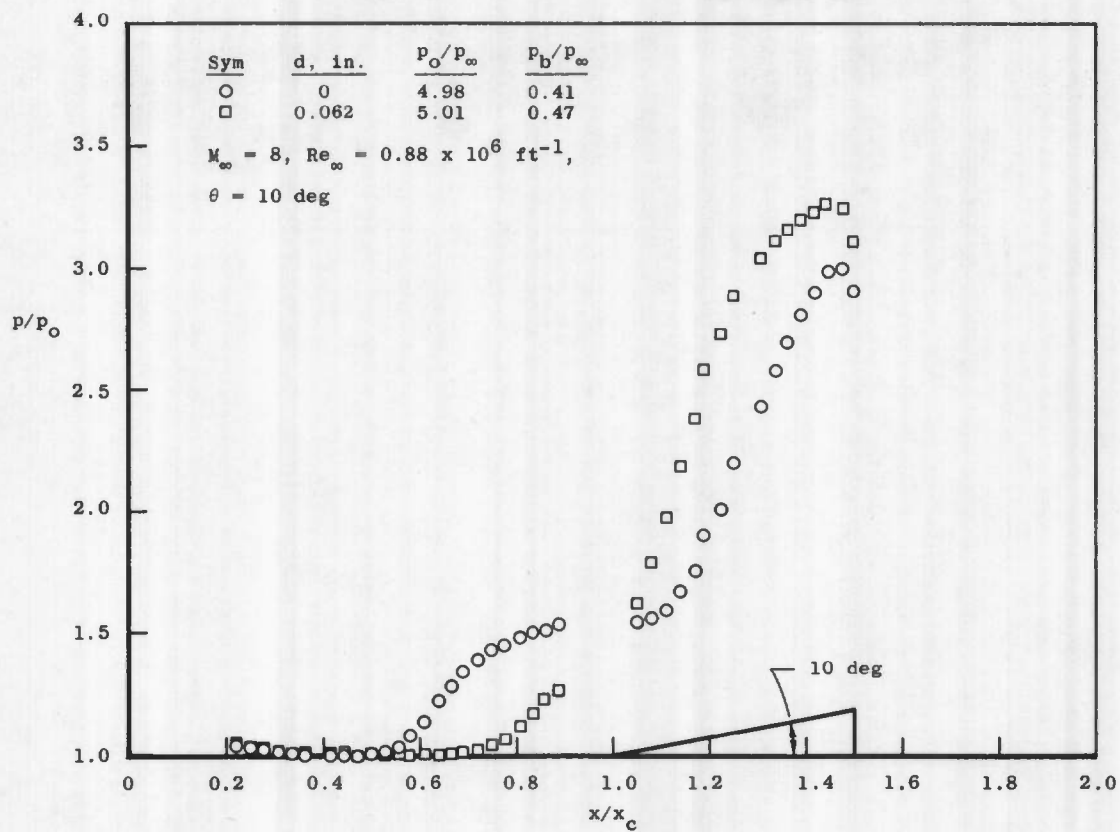
a. $Re_{x_c} = 1.0 \times 10^6$

Fig. 14 Effect of Mass Removal on Separation at $M_{w_1} = 6$
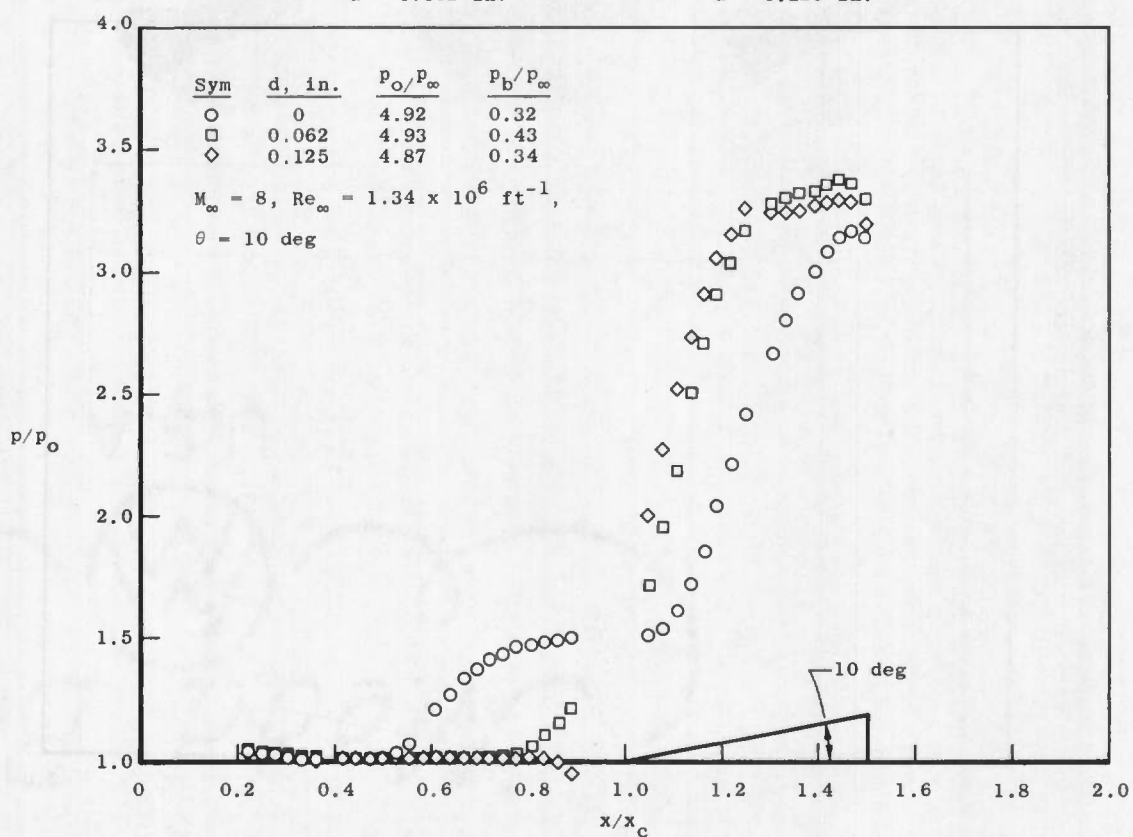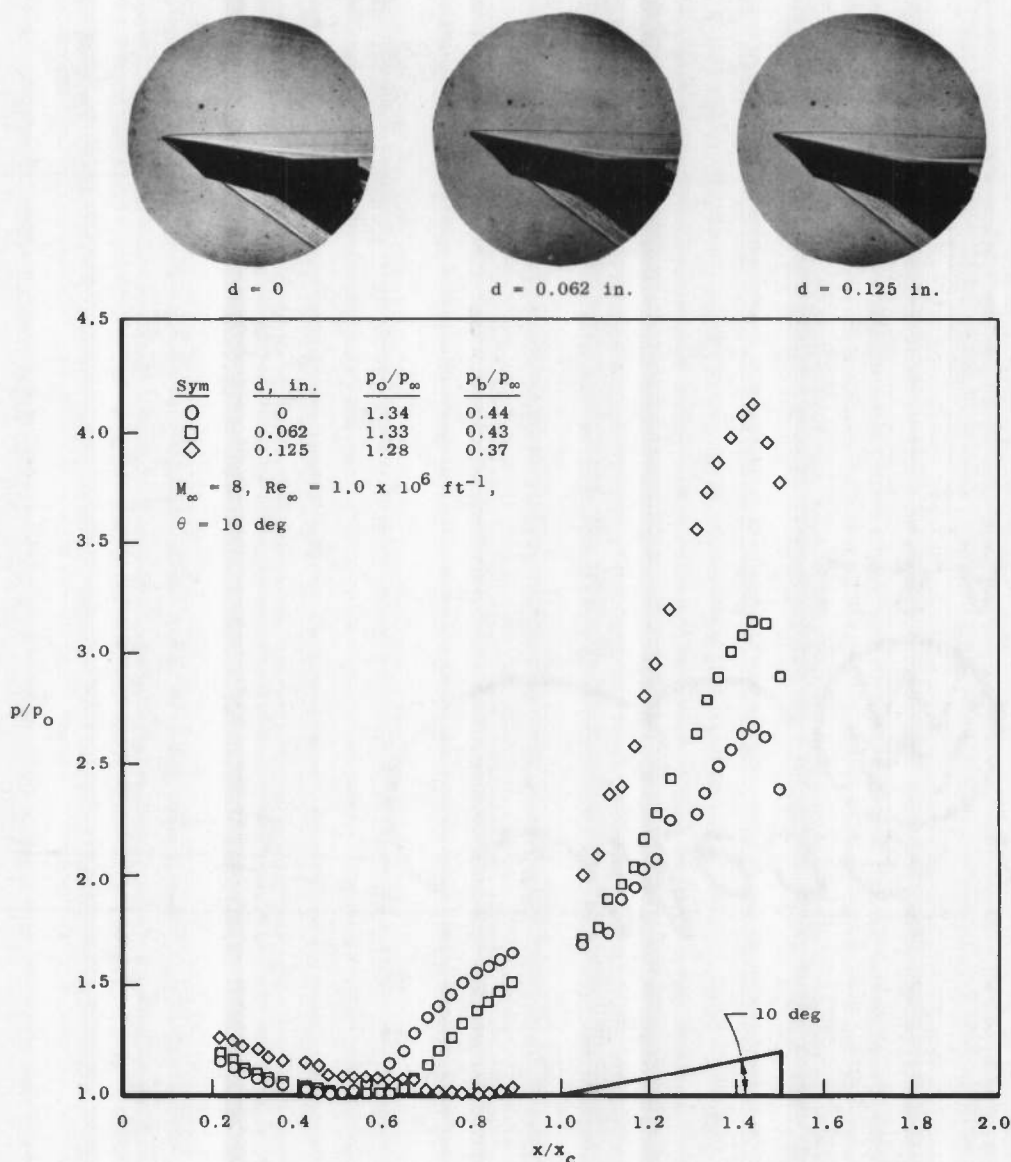
38

d = 0.062 in.   d = 0.125 in.


b. $Re_{x_c} = 1.5 \times 10^6$
Fig. 14 Concluded

39

The data obtained with the model at zero pitch (Fig. 15) appears, at least in the shadowgraph picture at the lower Reynolds number, to be laminar at reattachment. The separation region apparently was not completely removed at either Reynolds number, even with the slot opened to 0.125 in. (area = 2.225 in.^{2}), because a very slight pressure rise was present upstream of the slot (instead of the drop below a ratio of 1.0 as seen from the previous figures). These data suggest that the gap (bleed) area required to eliminate the upstream interaction increases with an increase in Mach number.

d = 0   d = 0.062 in.   d = 0.125 in.

Sym	d, in.	p_o/p_∞	p_b/p_∞
O	0	1.34	0.44
□	0.062	1.33	0.43
◇	0.125	1.28	0.37

$M_\infty = 8$, $Re_\infty = 1.0 \times 10^6$ ft^{-1}, $\theta = 10$ deg

a. $Re_{x_c} = 0.75 \times 10^6$

Fig. 15 Effect of Mass Removal on Separation at $M_{w_1} = M_\infty = 8$

d = 0   d = 0.062 in.   d = 0.125 in.
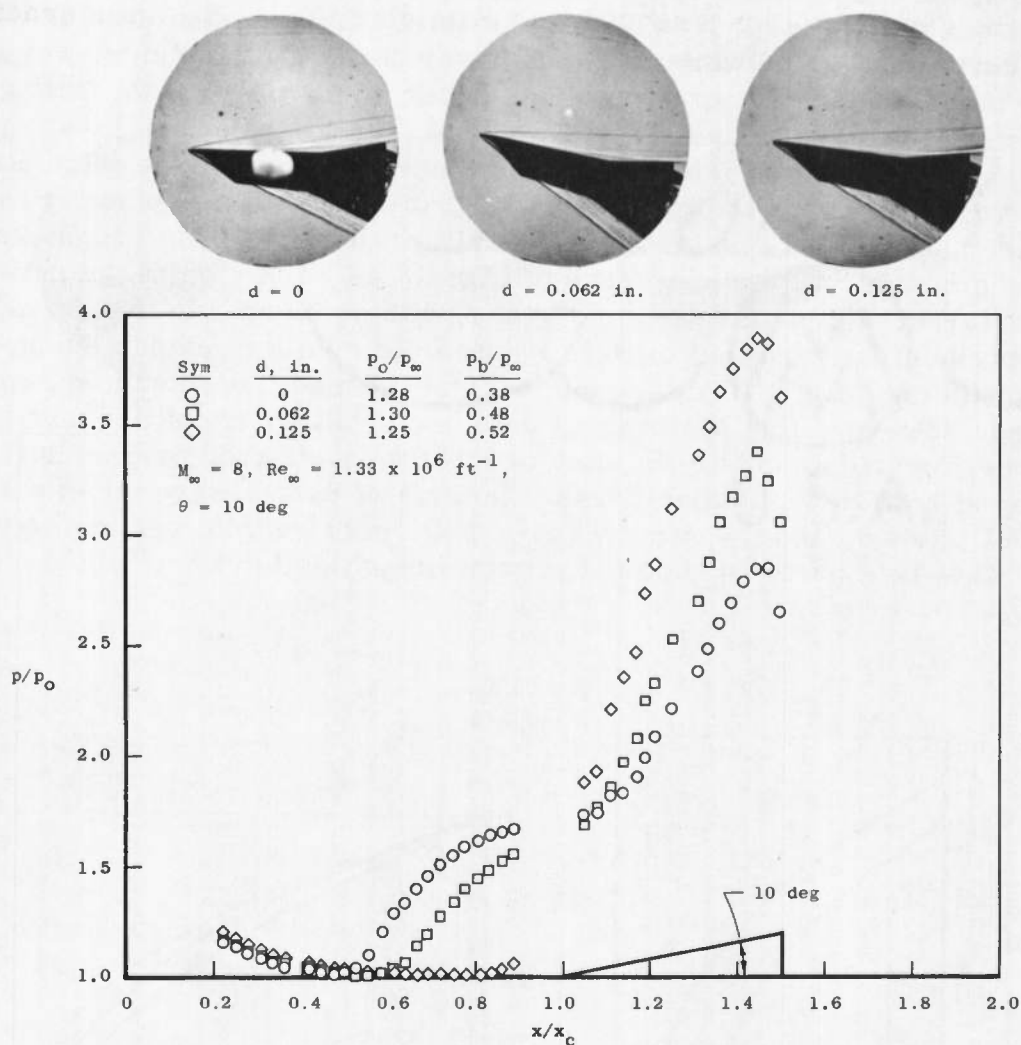
b. $Re_{x_c} = 1.0 \times 10^6$
Fig. 15 Concluded

41

Ball (Ref. 1) has obtained mass bleed data at several Mach numbers (M_{w_i} = 5.3, 6.5, 6.7, and 8.0) but with the model pitched at M_∞ = 12. These data were also all at different Reynolds numbers (Re_{x_c}). A comparison of the present data at $M_{w_i} = M_\infty = 8$ to those of Ball at $M_{w_i} = 8$, $M_\infty = 12$ is shown in Fig. 16. The weight flow was calculated in the same manner as Ref. 1, i.e., using the static pressure at the hinge line and the wall temperature as the supply conditions and by assuming sonic flow at the slot inlet. The present data on the left curve of Fig. 16 were extrapolated to obtain the amount of weight flow bleed needed for the "incipient" separation. The weight flow was ratioed to the theoretical weight flow in a laminar boundary layer on an adiabatic flat plate of length x_c. The theoretical value was calculated by integrating the velocity and density profiles (insulated plate, Prandtl number = 0.75) obtained from the results in Ref. 9. This weight flow ratio is shown in the right curve of Fig. 16 as a function of the ratio of the interaction length with bleed to that with no bleed. In this form, the present data and that of Ref. 1 appear to give a reasonable correlation with only slight Reynolds number dependence. It should be remembered, however, that the present data are probably transitional at the higher Reynolds number and may be adversely affected by the short ramp at both Reynolds numbers. The data of Ref. 1 were taken with the model pitched, and the ramp was, in fact, shorter with respect to the flat plate (x/x_c = 1.43) than the present investigations.
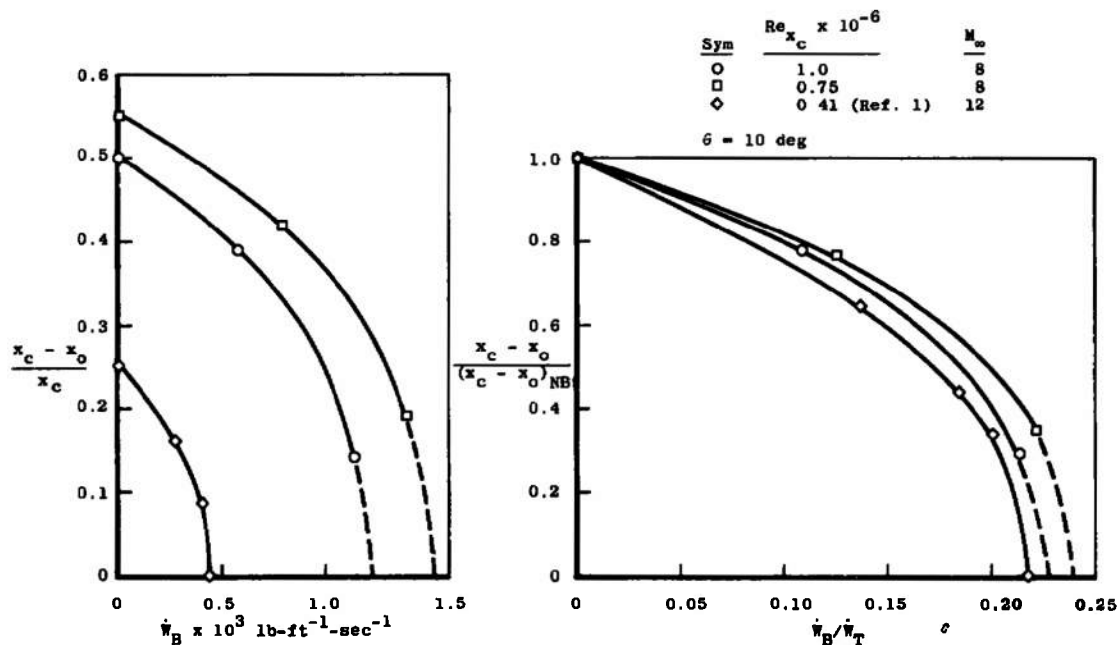

Fig. 16 Effect of Mass Removal on Interaction Length at M_{w_i} = 8

SECTION V
CONCLUDING REMARKS

Results of this investigation show that two-dimensional, ramp induced, laminar boundary-layer separations were obtained for Mach numbers 6, 8, and 10 at $Re_{x_C} = 0.38 \times 10^6$. The Mach number 6 data were found to be two-dimensional either with or without side plates; the Mach number 8 and 10 data were only judged two-dimensional with side plates (no Mach number 10 data were obtained without side plates). The boundary layer was probably laminar through reattachment at $Re_{x_C} = 0.38 \times 10^6$ or below for all three Mach numbers; however, there remains some question regarding the Mach number 6 data relative to that of other investigations.

At $M_\infty = 10$, a small change in the ramp angle (1 deg) was shown to give a large variation in both the upstream interaction and in the overall ramp pressure rise.

The data obtained during this investigation show large variations in the extent of upstream interaction and in the ramp pressure gradient between two sets of data obtained at the same local Mach number and Reynolds number but at different free-stream conditions. It was found that, even when local conditions were matched, valid separation data could not be obtained by pitching the model to obtain a lower Mach number.

From the limited amount of data obtained, it was found that the separation induced by a 10-deg ramp angle at Mach numbers 4.5 and 6 on a pitched flat plate was completely eliminated by removing mass from the separation region. In the case of the unpitched plate-ramp combination at $M_\infty = 8$, the data indicated that the separation could have been eliminated by removing between 20 to 25 percent of the theoretical weight flow in a laminar boundary layer on a flat plate of length x_C.

Because of the model failure during the tests, much of the investigation remains incomplete. Other investigators have also left several major points unresolved either because the flow in their experiments was not examined in sufficient detail for two-dimensionality, or checked closely for laminar flow at reattachment, or was not clearly free of geometry limitations. While quite a bit of data has been published on boundary-layer separation with mass removal, insufficient data are available to obtain a comprehensive understanding of the factors involved. The major points which require further investigation are (1) the validity of the separation data obtained with a flat-plate-ramp combination

pitched in order to obtain lower than free-stream local Mach numbers, (2) the effect of mass bleed on two-dimensional, laminar boundary-layer separation that is not limited by model geometry, (3) the cause of the discrepancy between the pressure gradient on the ramp obtained during the present tests and that predicted by adiabatic, integral-moment separation theory, and (4) the effects of flat-plate length and/or aspect ratio on the complete pressure distribution, particularly at Mach number 6.

REFERENCES

1. Ball, K. O. W. "Effects of Flap Length and Slot Suction on Laminar Boundary Layers." AIAA Paper 69-36, January 1969.

2. Gray, J. D. "Investigation of the Effect of Flare and Ramp Angle on the Upstream Influence of Laminar and Transitional Reattaching Flows from Mach 3 to 7." AEDC-TR-66-190 (AD645840), January 1967.

3. Ames Research Staff. "Equations, Tables, and Charts for Compressible Flow." NASA Report 1135, 1953.

4. Klineberg, J. M. "Theory of Laminar Viscous-Inviscid Interactions in Supersonic Flow." Ph. D. Thesis, California Institute of Technology, 1968.

5. Lees, L. and Reeves, B. L. "Supersonic Separated and Reattaching Laminar Flows: I. General Theory and Applications to Adiabatic Boundary Layer/Shock-Wave Interactions." AIAA Journal, November 1964.

6. Lewis, J. E. "Experimental Investigation of Supersonic Laminar, Two Dimensional Boundary Layer Separation in a Compression Corner with and without Cooling." Ph. D. Thesis, California Institute of Technology, 1967.

7. Ko, D. R. S. and Kubota, T. "Supersonic Laminar Boundary Layer along a Two-Dimensional Adiabatic Curved Ramp." AIAA Paper 68-109.

8. Ginoux, J. J. "Supersonic Separated Flows over Wedges and Flares with Emphasis on a Method of Detecting Transition." ARL 69-0009, January 1969.

9. Van Driest, E. R. "Investigation of Laminar Boundary Layer in Compressible Fluids Using the Crocco Method." NACA TN 2597, January 1952.

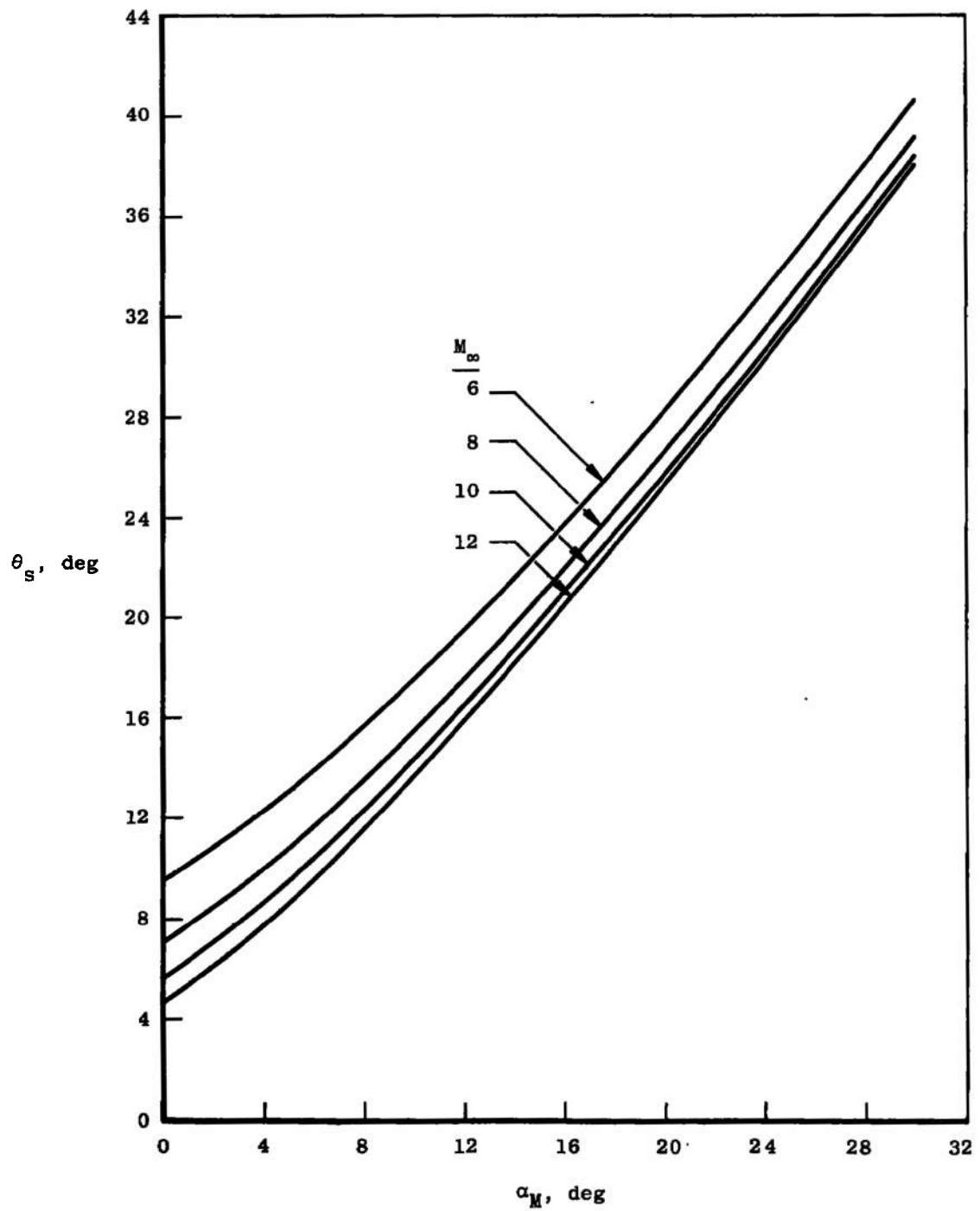**APPENDIX**
INVISCID WEDGE CURVES
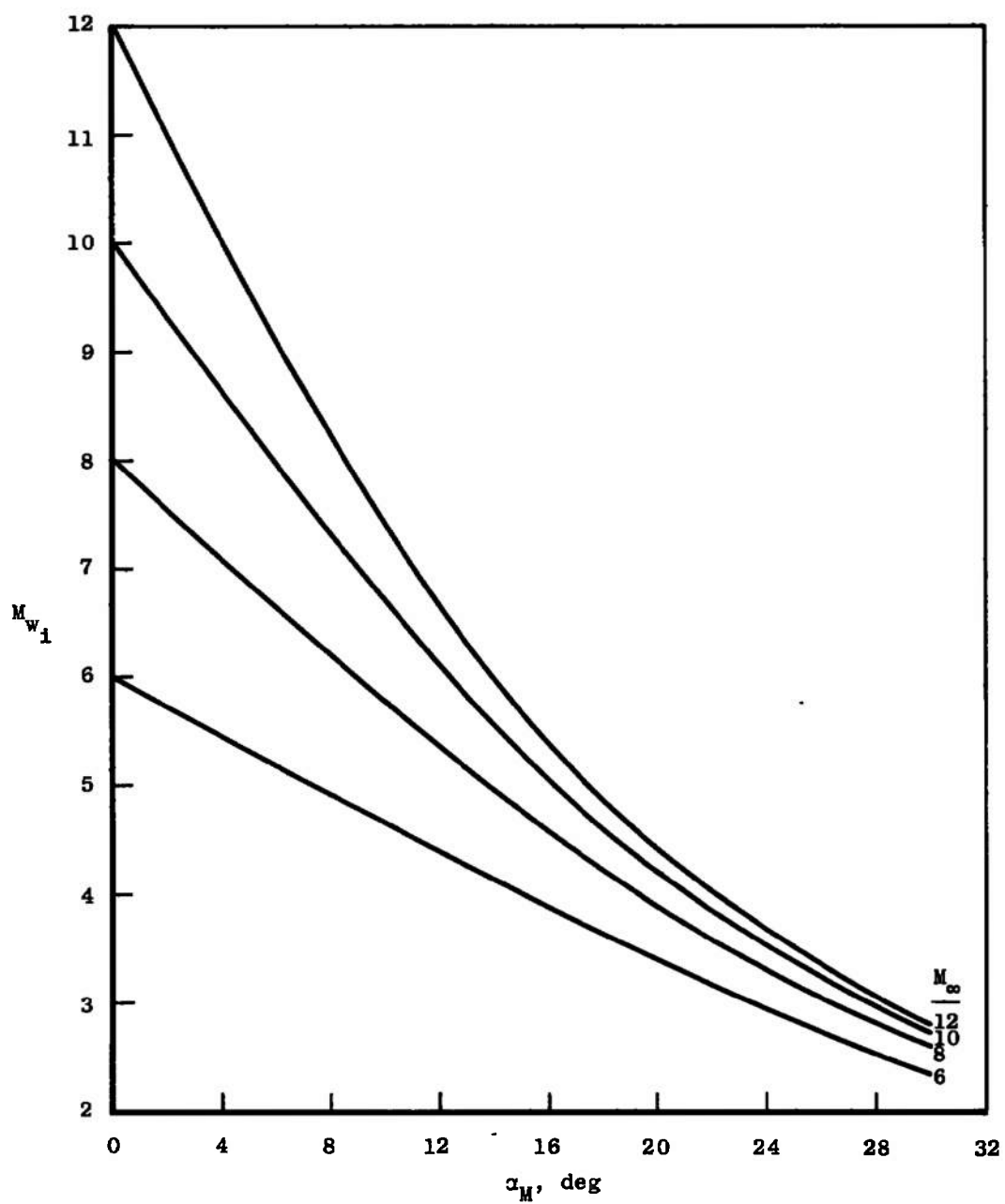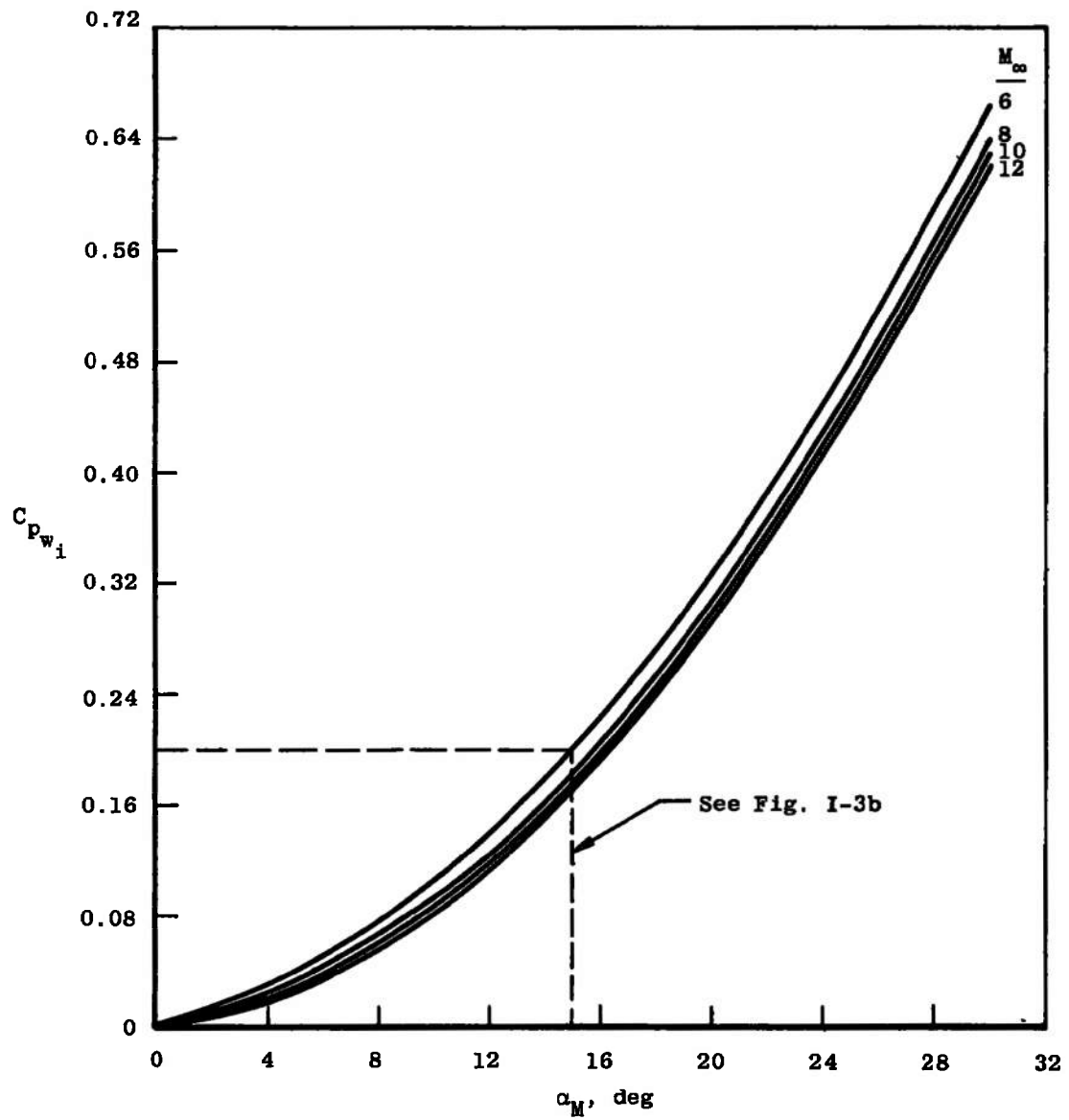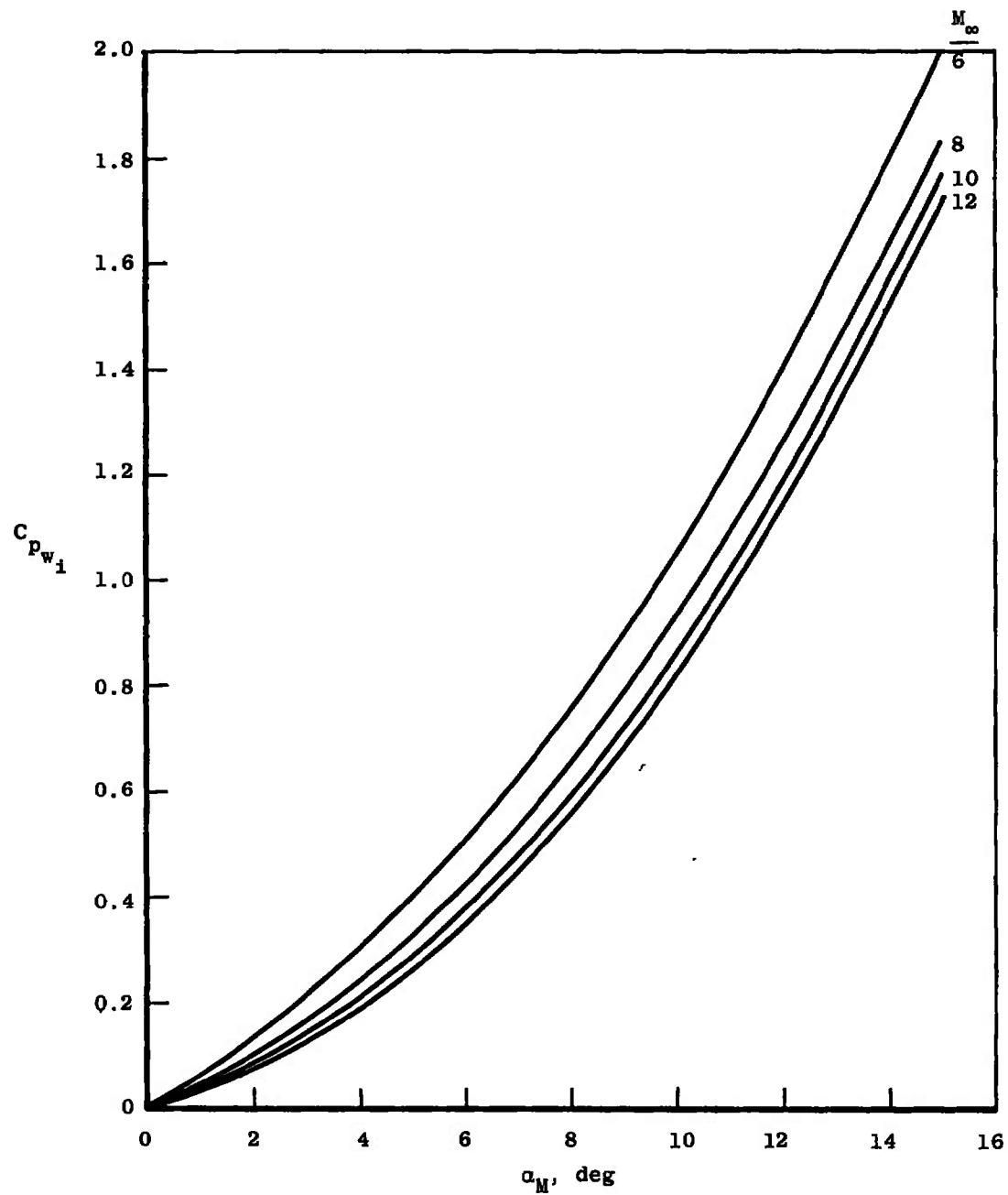
Fig. 1-1 Wedge Shock Wave Angle

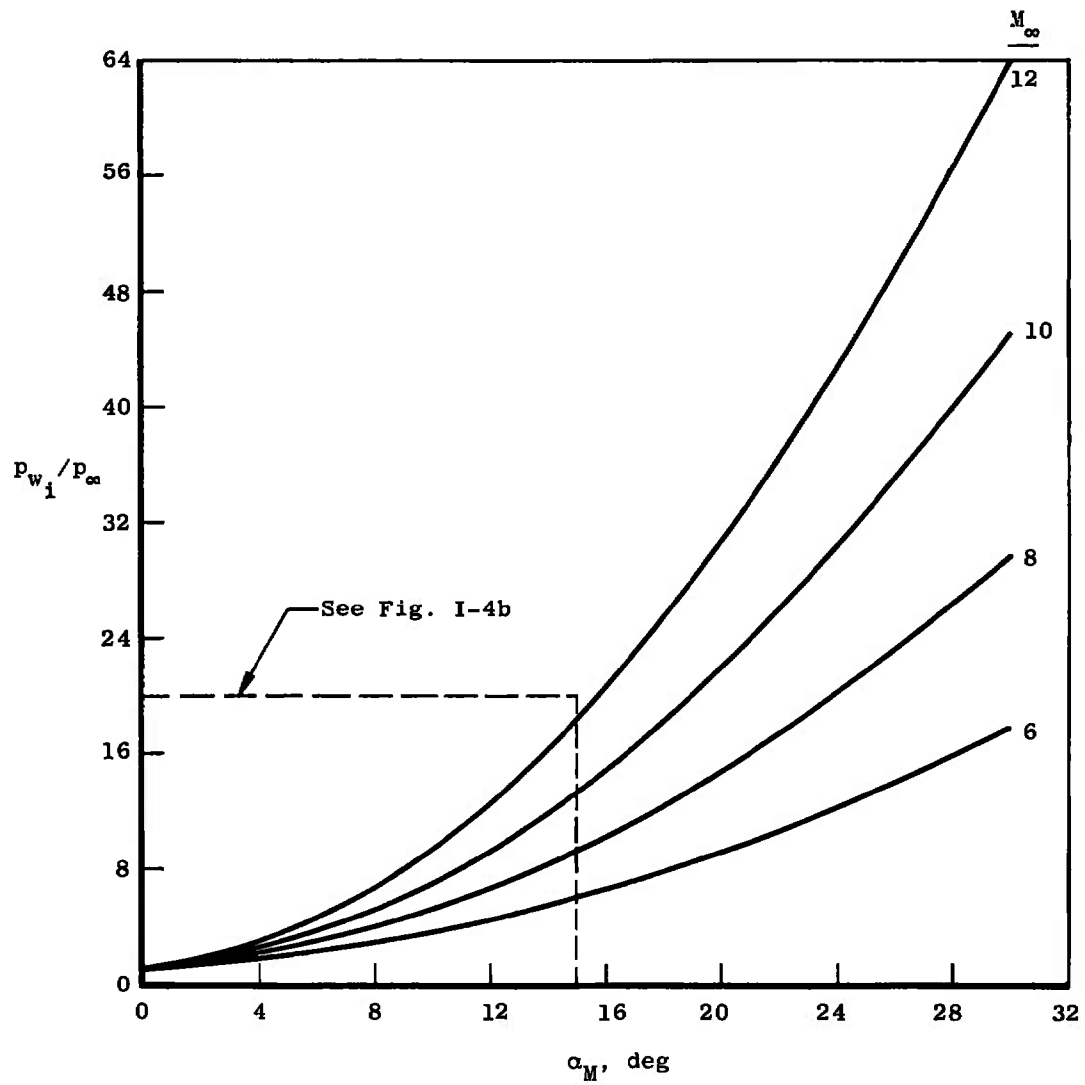**Fig. I-2 Wedge Surface Mach Number**

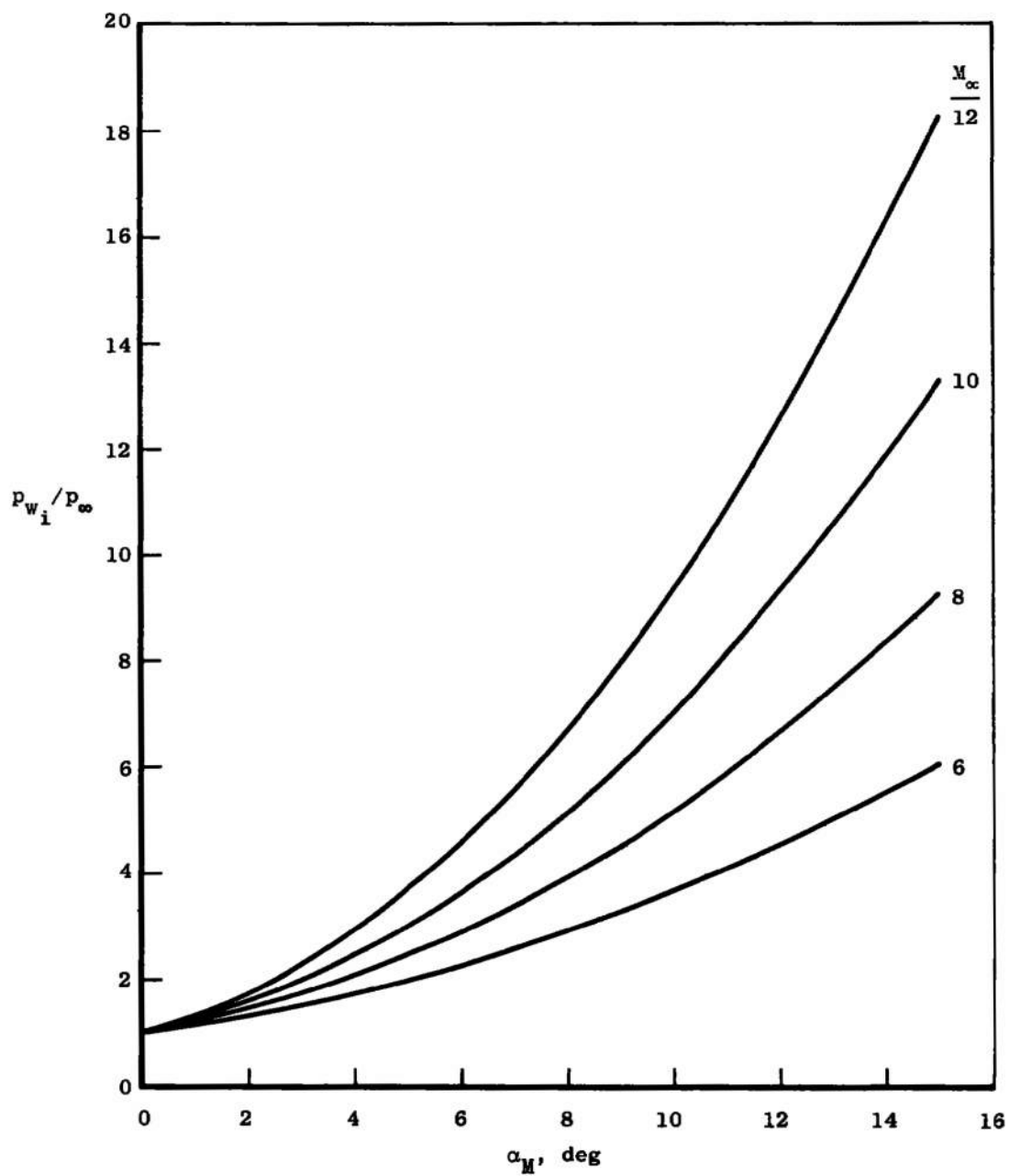a. $\alpha_M = 0$ to 30 deg

Fig. I-3 Wedge Surface Pressure Coefficient

b. $a_M = 0$ to 15 deg
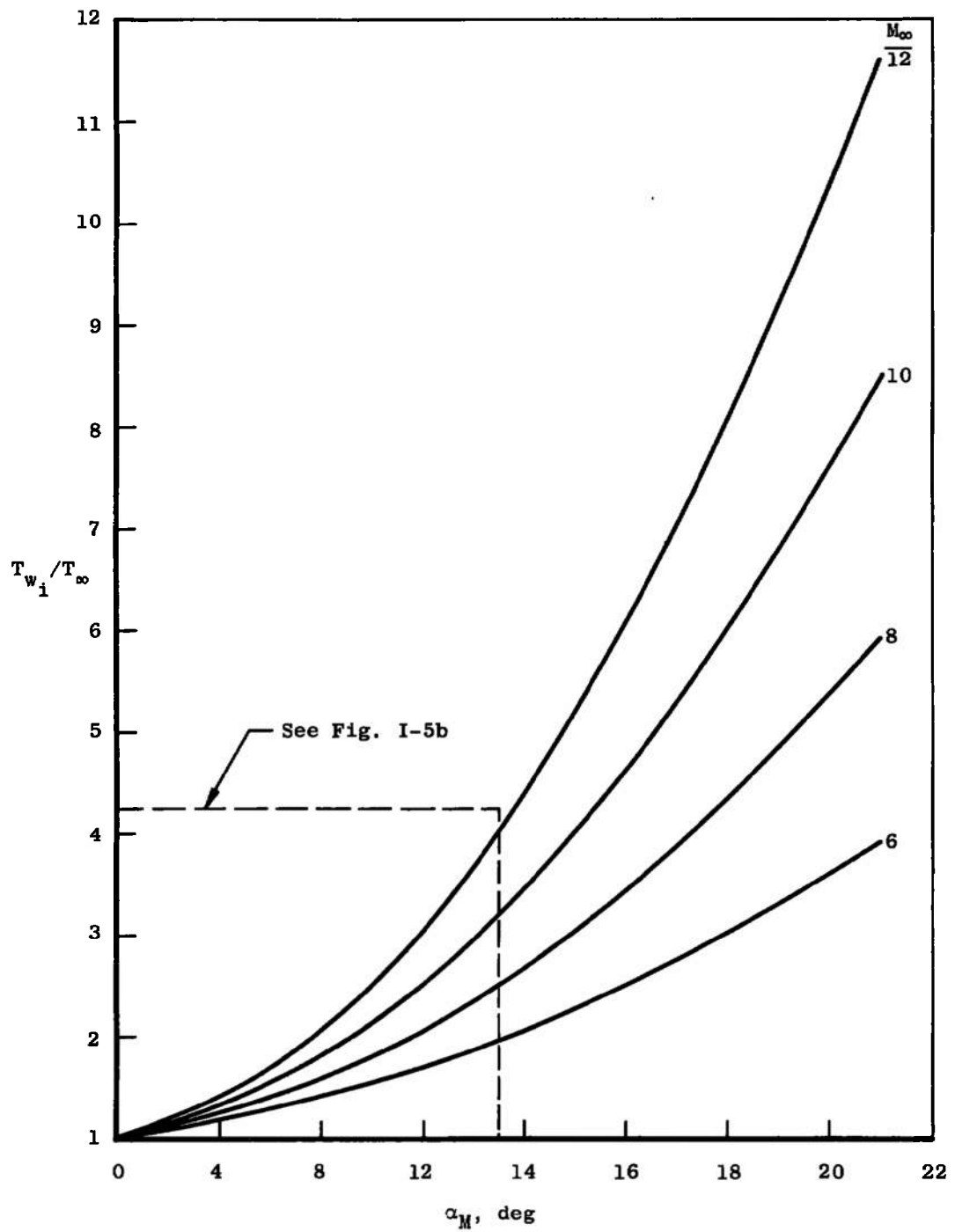
Fig. I-3 Concluded

a. α_M = 0 to 30 deg
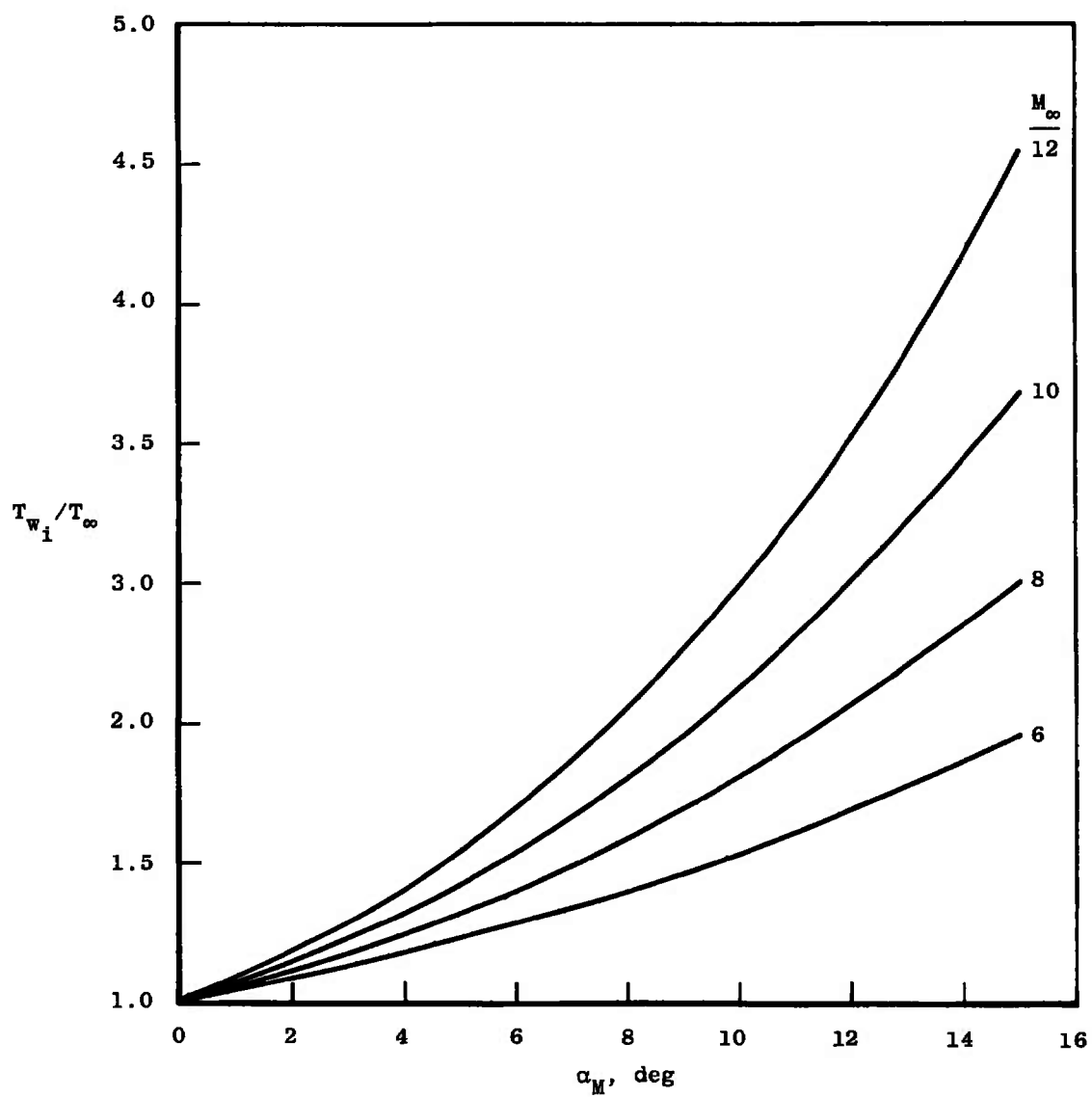
Fig. I-4 Wedge Surface Pressure Ratio

b. α_M = 0 to 15 deg
Fig. I-4 Concluded

a. α_M = 0 to 30 deg

Fig. I-5 Wedge Surface Temperature Ratio
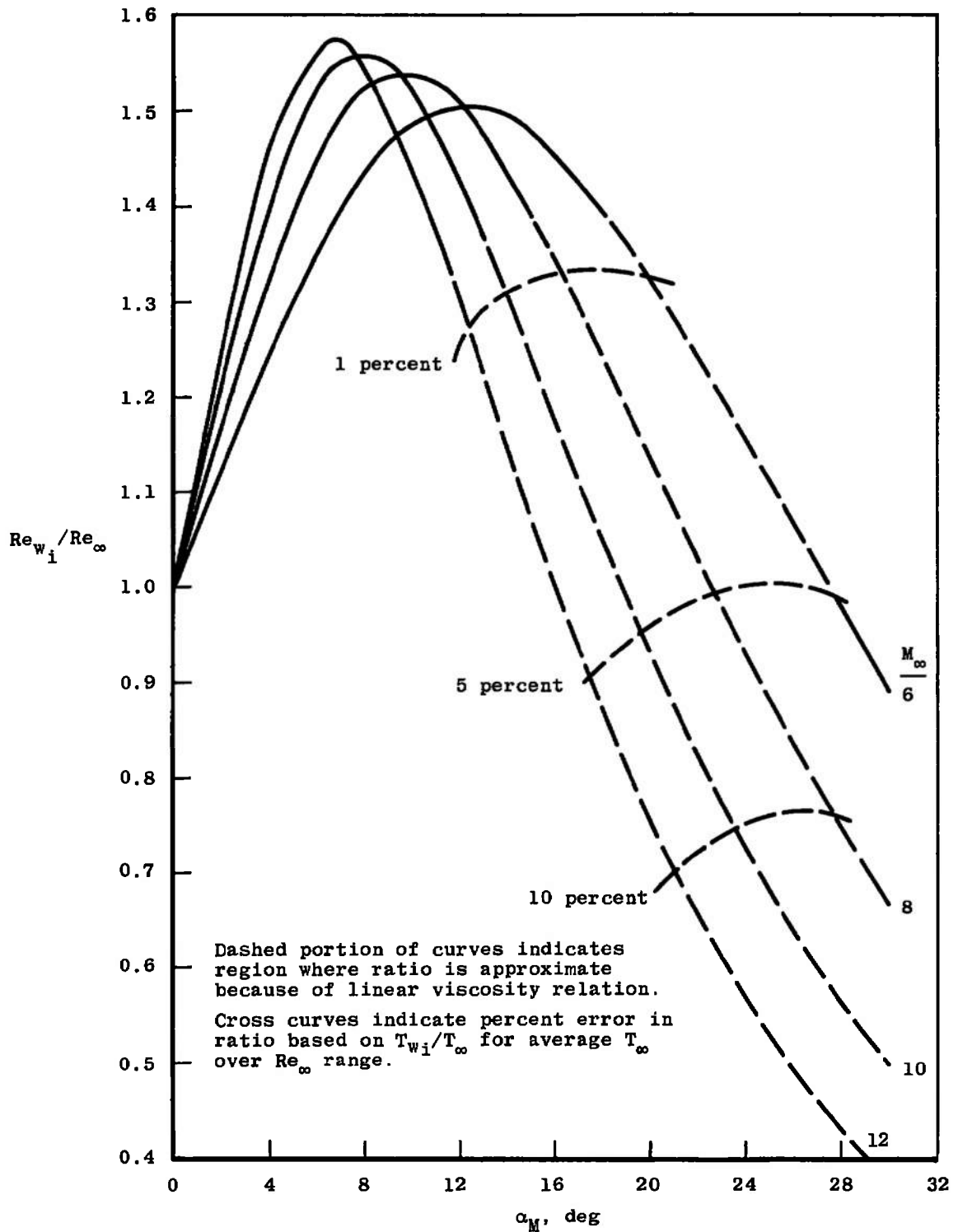
b. $\alpha_M = 0$ to 15 deg
Fig. I-5 Concluded

Fig. I-6 Wedge Reynolds Number Ratio

DOCUMENT CONTROL DATA - R & D

(Security classification of title, body of abstract and indexing annotation must be entered when the overall report is classified)

1. ORIGINATING ACTIVITY *(Corporate author)*	2a. REPORT SECURITY CLASSIFICATION
Arnold Engineering Development Center ARO, Inc., Operating Contractor Arnold Air Force Station, Tennessee 37389	UNCLASSIFIED
	2b. GROUP N/A

3. REPORT TITLE

INVESTIGATION OF LAMINAR BOUNDARY-LAYER SEPARATION ON A FLAT-PLATE-RAMP COMBINATION WITH AND WITHOUT MASS REMOVAL AT MACH NUMBERS 6, 8, AND 10

4. DESCRIPTIVE NOTES *(Type of report and inclusive dates)*

July 11, 1965 to April 18, 1969 - Final Report

5. AUTHOR(S) *(First name, middle initial, last name)*

R. W. Rhudy, ARO, Inc.

6. REPORT DATE	7a. TOTAL NO. OF PAGES	7b. NO. OF REFS
March 1970	63	9

8a. CONTRACT OR GRANT NO. F40600-69-C-0001	9a. ORIGINATOR'S REPORT NUMBER(S)
b. PROJECT NO. 1366	AEDC-TR-69-199
c. Program Element 62201F	9b. OTHER REPORT NO(S) *(Any other numbers that may be assigned this report)*
d.	N/A

10. DISTRIBUTION STATEMENT

This document has been approved for public release and sale; its distribution is unlimited.

11. SUPPLEMENTARY NOTES	12. SPONSORING MILITARY ACTIVITY
Available in DDC.	Arnold Engineering Development Center, Air Force Systems Command, Arnold AF Station, Tennessee 37389

13. ABSTRACT

An experimental investigation of laminar boundary-layer separation induced by a trailing edge ramp on a flat plate was conducted at Mach numbers of 6, 8, and 10. The tests were conducted over a range of Reynolds numbers. Longitudinal and spanwise surface pressure distributions, pitot pressure profiles, and shadowgraph pictures were used to investigate the two-dimensionality of the flow and the effects of model geometry, angle of attack, Reynolds number, ramp angle, and mass removal from the separation region. Data are presented to show that laminar, two-dimensional boundary-layer reattachment, not limited by model geometry, was obtained. These data are compared to the integral-moment theory of Lees and Reeves as modified by Klineberg. It is also shown that a separation region can be reduced or even eliminated by removing mass at the hinge line.

DD FORM 1473 1 NOV 65

14. KEY WORDS	LINK A		LINK B		LINK C	
	ROLE	WT	ROLE	WT	ROLE	WT
boundary-layer separation						
laminar boundary layer						
trailing edges						
ramps						
flat plate models						
two-dimensional flow						
hypersonic flow						